**Ricardo Lima Pereira**
Licenciatura em Ciências da Engenharia Química e Bioquímica

# Aptamers Binding to Bradykinin

Dissertação para obtenção do Grau de Mestre em
Bioquímica para a Saúde

Orientador: Prof. Doutor Alexander Henning Ulrich, Instituto de Química da Universidade de São Paulo

**Junho de 2015**

**Ricardo Lima Pereira**
Licenciatura em Engenharia Química e Bioquímica

# Aptamers Binding to Bradykinin

Dissertação para obtenção do Grau de Mestre em
Bioquímica para a Saúde

Orientador: Prof. Doutor Alexander Henning Ulrich, Instituto de Química da Universidade de São Paulo
Elo de Ligação: Prof. Doutor Michel Kranendonk, Nova Medical School - Universidade Nova de Lisboa

Júri:

Presidente: Prof. Doutora Maria Teresa Nunes Mangas Catarino
Arguente: Prof. Doutora Ana Luísa Ferreira Simplício
Vogais: Prof. Doutora Ana Luísa Ferreira Simplício
Prof. Doutor Alexander Henning Ulrich

**Faculdade de Ciências e Tecnologia da Universidade Nova de Lisboa**

**Junho de 2015**

*The work presented in this MSc dissertation was done at the Neurosciences Lab within the Chemistry Institute of the University of São Paulo.*

**Acknowledgements / Agradecimentos**

Em primeiro lugar, quero agradecer ao meu orientador- Professor Henning Ulrich- por ter apostado em mim. Ao abrir as portas do seu laboratório abriu-me, também, as portas da ciência e de um futuro novo e promissor, repleto de crescimento profissional e pessoal- um gesto que relembrei e tentei retribuir em cada passo deste projecto.

Um agradecimento, também, ao Professor Doutor Michel Kranendonk por ter feito a ponte entre as duas instituições- FCT-UNL e IQ-USP- e entre os dois países; um gesto que me permitiu "trabalhar em casa fora de casa".

Quero, também, agradecer aos meus colegas e amigos Arquimedes, Claudiana e Ana Paula, pelo companheirismo, pelo carinho e pelo esforço incansável durante todo o processo científico que levou à aprimoração deste trabalho- ele é tanto meu como vosso!

Agradeço, também, aos restantes colegas e amigos do laboratório pela amizade, pela receptividade e, acima de tudo, pela paciência para os meus devaneios!

Não podia deixar de agradecer ao IQ-USP por me aceitar como aluno e permitir a execução deste trabalho e à FCT-UNL; em particular, aos Professores Teresa Catarino, Sebastião Rodrigues, Pedro Matias e Ricardo Franco: a concepção deste mestrado foi uma iniciativa extraordinária e a proximidade com que acompanharam esta primeira "remessa" de alunos revelou um profissionalismo e dedicação exímios.

Agradeço, também, aos meus amigos (vocês sabem quem são!) que ficaram em terras lusas e que nunca deixaram de manifestar o seu apoio nesta grande mudança; assim como à "nova família" que encontrei no Brasil- Ana, Pedro e Cris (a força motriz!)- que todos os dias cimenta a convicção de que esta mudança foi para melhor.

Por último, mas não menos importante, quero agradecer às três pessoas mais importantes ao longo deste processo- aquelas que me deram e dão, dia após dia, a força para construir o dia seguinte:

- a minha namorada; amiga e companheira de todas as horas
- a minha querida irmã; a outra metade de quem sou
- o meu pai; pai, amigo e mentor.

*Para o meu pai:*

*não importa como se começa, mas sim como se acaba.*

*Everything has been figured out, except how to live.*

Jean-Paul Sartre.

**Abstract**

Bradykinin is a peptide of the kinin group, involved in a number of receptor-mediated physiological actions, including inflammation and vasodilation, as well as neuromodulation, neuroprotection and promotion of neurogenesis.

Bradykinin is the main ligand of the B2 receptor- the main kinin receptor- which is involved in the cardiac and renal protective effects of kinins in diseases. Antibodies have been considered for a long time as promising therapeutic agents in various fields, especially cancer-related ones. Aptamers, on the other hand, have proven to be an excellent alterative, since they have similar properties to those of monoclonal antibodies, such a high-specificity of recognition and high-affinity binding. Plus, they are developed using *in vitro* selection procedures and can be reproduced by enzymatic reactions. SELEX is a powerful tool for the development of both DNA and RNA aptamers. The main goal of this project was to design a method to select aptamers against bradykinin using capillary electrophoresis alongside the SELEX technique. The selection was done by comparing the aptamers' (ssDNA-target complex) electrophoretic mobility with that of the ssDNA and the target, which allowed us to define an appropriate collection window that took into consideration the analytes' detection time, thus enabling the collection of the desired oligonucleotides. After two selection rounds, the collected pool was sequenced, the affinity was measured and the aptamers' secondary structure was predicted.

We concluded that with only two selection cycles, the original DNA library's bulk affinity grew around 0.4%. The structural characterization of the aptamers, performed with the aid of the Mfold software, revealed that there are many repetitive motifs amongst them, indicating that the selection process was successful.

We have obtained 16 sequences of candidate aptamers as bradykinin ligands of similar sequences and secondary structures whose biological activity should be analyzed after synthesis; mainly in regard to their role as bradykinin inhibitors.

**Key words:** Bradykinin, Kinins, Aptamers, SELEX, DNA, Capillary Electrophoresis.

**Resumo**

A bradicinina é um péptido pertencente ao grupo das cininas que está envolvido em várias acções fisiológicas: desde inflamação e vasodilatação a processos de neuromodulação e neuroprotecção. É, também, o ligando principal do receptor B2- o receptor principal das quininas, que está envolvido nas suas acções protectoras em doenças renais e cardíacas.

Tanto os anticorpos monoclonais como os aptâmeros sintetizados através da química combinatória têm vindo a ser desenvolvidos como drogas de acção *in situ*. Durante muito tempo, os anticorpos foram considerados ferramentas terapêuticas com um potencial elevadíssimo. Já os aptâmeros, por sua vez, têm-se vindo a revelar uma óptima alternativa, por possuírem maior especificidade e afinidade e serem simples de sintetizar, além de poderem ser desenvolvidos contra qualquer alvo. O SELEX é uma ferramenta poderosíssima no que toca ao desenvolvimento de aptâmeros. O objectivo principal deste projecto foi desenvolver um método de selecção de aptâmeros contra a bradicinina através do acoplamento da electroforese capilar à já conhecida técnica de SELEX.

A selecção dos aptâmeros foi efectuada por comparação das suas mobilidades electroforéticas (ou seja, da mobilidade electroforética do complexo ssDNA-alvo) com aquelas da biblioteca de DNA inicial e a do alvo. Esta comparação permitiu deifnir uma janela temporal adequada para colecta dos oligonucleótidos pretendidos. Depois de efectuados dois ciclos de selecção, a *pool* seleccionada foi sequenciada e a sua afinidade pelo alvo foi medida. Concluímos que, com apenas dois ciclos de selecção, a afinidade dos oligonucleótidos aumentou em 0.4%. A análise da sua estrutura secundária através do programa Mfold permitiu identificar motivos muito semelhantes entre as sequências obtidas, o que demonstra uma selecção bem sucedida, na qual se obtiveram 16 sequências com constituição e estrutura semelhantes cuja actividade biológica face à inibição daquela da bradicinina deve ser analisada depois de sintetizados os aptâmeros.

**Palavras chave:** Bradicinina, Cininas, Aptâmeros, SELEX, DNA, Electroforese Capilar

## Contents

**Figures**

**Tables and Equations**

**Abbreviations**

Bk- bradykinin

CE- Capillary Electrophoresis

EOF- Electroosmotic flow

Arg- Arginine

Pro- Proline

Gly- Glycine

Phe- Phenilalanin

Ser- Serine

Des-Arg9- Des-Arginine-9

Bk 1-5- the 1-to-5 amino acid fragment of bradykinin (Arg-Pro-Pro-Gly-Phe)

ACE- Angiotensin-Converting-Enzyme

B2BkR- B2 Bradykinin Receptor

HOE 140 (a Bk inhibitor also known as icatibant acetate, firazyr or JE 049)- D-Arg-L-Arg-L-Pro-L-Hyp-Gly-L-(2-thienyl)Ala-L-Ser-D-1,2,3,4-tetrahydro-3-isoquinolinecarbonyl-L-(2α,3β,7aβ)-octahydro-1H-indole-2-carbonyl-L-Arg

iPS- Induced Pluripotent Stem Cells

CNS- Central Nervous System

SELEX- Systematic Evolution of Ligands by Exponencial Enrichment

DNA- Deoxyribonucleic Acid

RNA- Ribonucleic Acid

PEG- Polyethylene Glycol

ATP- Adenosine Try-Phosphate

VEGF- Vascular Endothelium Growth Factor

PCR- Polymerase Chain Reaction

HPLC- High Pressure Liquid Chromatography

KCE- Kinetic Capillary Electrophoresis

NECEEM- Non-Equilibrium Capillary Electrophoresis of Equilibrium Mixtures

CE-SELEX – Capillary Electrophoresis-SELEX

ssDNA- Single-Stranded DNA

dsDNA- Double-Stranded DNA

CD73- Cluster of Differentiation 73

DAD- Diode Array Detector

LIF- Laser Induced Fluorescence

# Chapter 1

## Introduction

### 1.1. Aptamers and SELEX- Promising Tools in Treatment and Diagnostics

Today, combinatorial chemistry is one of the most promising tools at the pharmaceutical industry's disposal, when it comes to discovering and developing new therapeutic molecules.

In a glance, its use consists in three steps: synthesizing a new and random molecular library, selection against a specific target and finally and characterizing the newly formed ligand-target complex.

Nucleic acids are, definitely, compounds of interest in this field, because not only do they fold into well-defined secondary and tertiary structures but, also, are easy to synthesize[1]. With that in mind, in 1990, Tuerk, Gold, Ellington and Szostak developed a technique that allows the isolation of nucleic acid molecules from a library with over $10^{15}$ sequences. That technique was then called SELEX (*Systematic Evolution of Ligands by EXponential Enrichment*) and those molecules, aptamers (from *aptus*, in latin, which means "on/snap")[2, 3]. SELEX can also be referred to as *in vitro selection* or *in vitro evolution*. It is a combinatorial chemistry technique used to produce oligonucleotides of either RNA or single-stranded DNA that specifically bind to a particular target [2, 4].

This technique allows (and has been put to that use) the selection of aptamers with high specificity and selectivity for a variety of targets, including small molecules such as ATP[5], adenosine[6,7] and proteins such as prions[8], as well as vascular endothelial growth factor (VEGF)[9]. However, there is no common protocol selection to all targets. The design of the SELEX procedure depends on the target, the oligonucleotide library, the application as well as the type of aptamer one intends to create.

The starting point for the SELEX technique is the synthesis of a library of single-stranded DNA (ssDNA, single-stranded DNA) containing about $10^{15}$ different sequences. Each sequence has a random region with 16 to 75 positions flanked by two constant regions, where primer annealing occurs, as well as digestion with restriction enzymes.

This chemically synthesized DNA is then enzymatically amplified using the polymerase chain reaction (PCR). After this, the double-stranded reaction product generated is denatured to a pool of single-stranded DNA oligonucleotides (ssDNA). The ssDNa is then submitted to specific temperature variations in specific time-frames in order to adopt two- and three-dimensional arbitrary structures that take advantage of the complementarity between its base pairs. This process is called DNA folding, and is crucial to enable the interaction between the ssDNA and the target during incubation. After the folding process, the ssDNA is then exposed to its target in order to select the sequences that constitute the desired aptamers[10].

The ssDNA pool is incubated with its selection target and the best fitting molecules are collected and amplified using PCR procedures. Reiterative SELEX rounds are performed with increasing stringency to ensure the identification of the binders with the highest affinity[10].

It is, in its essence, an evolutionary process consisting in variation, selection and replication[2]. And also a lengthy one, since it can take up to 20 cycles to obtain the desired affinity[11].

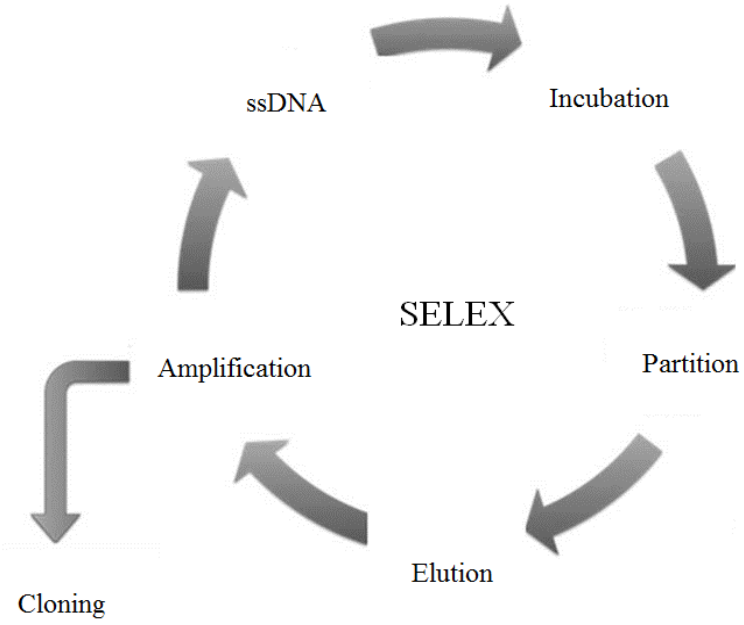


**Figure 1 - Schematic representation of the SELEX procedure used to obtain DNA aptamers.**

Since the inception of this technique, both DNA and RNA aptamers have been selected against various targets – ions, small molecules or even membrane receptors- and have demonstrated both affinity and specificity that pairs with that of monoclonal antibodies[12, 13].

Both monoclonal antibodies and combinatorial synthesized aptamers are being developed as site-specific drugs to bind to specific proteins that reveal altered activities in disease states. Antibodies have been considered for a long time as promising therapeutic agents in various fields, especially cancer-related ones[14].

Aptamers, however, have proven to be an excellent alternative, since they have similar properties to those of monoclonal antibodies, such a high-specificity of recognition and high-affinity binding. Plus, they are developed using *in vitro* selection procedures, can be developed against almost every target, do not require *in vivo* selection during their development and can be truncated to small biological-active sequences and modified for optimization[10, 9, 15].

Aptamers are nucleic acid or peptide molecules that bind to a specific target molecule and living cells with high affinity and specificity, making them promising affinity ligands and distinct tools as affinity probes and analytical and therapeutic reagents[16, 17, 18, 19]

Aptamers are usually created by selecting them from a large random sequence pool, but natural ones are also available in riboswitches (regulatory segments of a messenger RNA molecule that

bind a small molecule, resulting in a change in production of the proteins that it encodes-autoregulated mRNA[20, 21, 22]) and can be used for both basic research and clinical purposes as macromolecular drugs. Also, they can be combined with ribozymes to self-cleave in the presence of their target molecule.

Aptamers are useful in biotechnological, therapeutic and/or diagnostic applications as they offer molecular recognition properties that rival that of the commonly used biomolecules-antibodies[23, 9]. In addition to their discriminative recognition, aptamers offer advantages over antibodies as they can be engineered completely in a test tube, are readily produced by chemical synthesis, possess desirable storage properties and elicit little or no immunogenicity in therapeutic applications.

Non-modified aptamers are cleared rapidly from the bloodstream, with a half-life of minutes to hours, mainly due to nuclease degradation and clearance from the body by the kidneys, a result of the aptamer's inherently low molecular weight[15]. Unmodified aptamer applications currently focus on treating transient conditions such as blood clotting, or treating organs such as the eye where local delivery is possible. This rapid clearance, alongside the already mentioned high selectivity and affinity, represent advantages in applications such as *in vivo* diagnostic imaging. A good example is the tenascin-binding aptamer under development by Schering AG for cancer imaging.

Their high binding affinity and specificity, among other characteristics, has made them attractive diagnostic applications to target intra- and extracellular components of key signaling pathways[24]. One such example is the already known RNA aptamer against the epidermal growth factor receptor (EGFR), which allows detection and/or extent of glioblastoma multiforme[24].

Also, aptamers have been recently used as immobilized ligands or in homogeneous assays. Several important aspects have to be examined in details when using aptamers as immobilized ligands, such as the immobilization process[25]. Several findings demonstrated that aptamers could be differently susceptible to assay protocols and that optimal operating conditions could be different from one aptamer to another[26].

If all these important aspects are taken into consideration, the application of aptamers as bio-components in diagnostic assays offers a multitude of advantages, such as the possibility of easily regenerating the function of immobilized aptamers and the possibility of using different detection methods due to easy labelling[25].

Aptamers have been already been proposed as diagnostic tools for detection of cytokines and growth factors[27, 28] as well as thrombin, the last enzyme protease involved in the coagulation cascade which plays a central role in a number of cardiovascular diseases[29]. In fact, many assays based on the thrombin-binding aptamer for the detection of thrombin have been developed in the last 10 years[30, 31].

They have also been successfully used in proteomics and development of bioanalytical assays[32], inhibition of enzymes and receptors[33, 34], development of ribozymes and aptazymes[35], target validation and screening for drug candidates[36, 37]. In fact, their potential is so big that applications include gene therapy and drug delivery to therapeutic targets[38]. Their reputation grew immensely in the past years and they're considered promising tools in the treatment of various pathologies[39] and some are actually undergoing pre-clinical trials[40].

### 1.2. Capillary electrophoresis

Electrophoresis is the process of separating charged molecules (analytes) under the influence of an electric field.

Capillary electrophoresis (CE) is a relatively new and powerful separation technique that has taken essential components from both HPLC and electrophoresis.

In CE methods, analytes migrate through electrolyte solutions under the influence of an electric field inside a capillary tubing and, during this process, they can be separated according to ionic mobility. This technique can be viewed as an instrumental approach to electrophoresis and is ideally suited for handling *small* amounts of sample material to be analyzed and/or separated under the influence of such field.

The ability to analyze such small amounts of sample material is in high demand; a demand that becomes increasingly prominent in bioanalytical research, *e.g.*, in biotechnology and in various clinical, diagnostic and genetic applications.

Preceding modern CE, it is interesting to note that, as early as 1953, some experimenters recognized the importance of dealing with certain biological samples using the smallest apparatus available. For example, ribonucleotides could be identified in single cells using "micro-electrophoresis" in fine silk fibers (Edstrom, 1953).

CE takes advantage of two types of driving forces- the force causing the electrophoretic migration and the force exerted by the electroosmotic flow (EOF) through the capillary.

The EOF bulk flow results from the charged inner capillary wall during application of an electric field (Figure 2) [41].

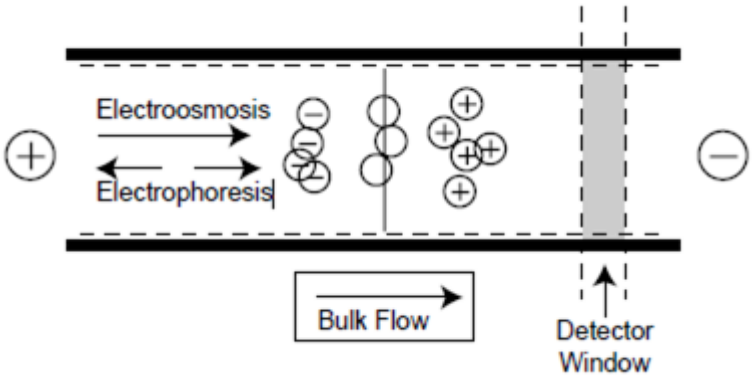


**Figure 2 - Depiction of electrophoresis and electroosmosis in a separation of anionic, neutral, and cationic analytes**. The injection takes place in the far left side of the capillary and the outlet is on the far right[41].

The analyte's migration rate, or apparent mobility, depends on the applied electric field (V) and its own specific mobility (μ), which is constant for a given set of conditions, as depicted in Equation 1 (where L is the length along which the voltage is applied and μ is the sum of the analyte's electroosmotic and electrophoretic mobility).

**Equation 1 - Migration rate**

$$V=\mu\bullet(V/L)$$

Given the fact that the capillary has a high surface to volume ratio, the applied voltage is far higher than the one used in other electrophoretic techniques, however, there are limits to consider, given the fact that, even though the capillary can be cooled down, it still caves when submitted extremely to voltages.

With untreated fused silica tubing and an aqueous buffer such as NaOH, a negatively charged capillary surface is obtained. The magnitude of the EOF depends on various experimental factors, most notably the pH of the buffer solution. Capillary coatings can reverse, reduce, or even totally eliminate the EOF[41]. The type of buffer and both its ionic strength and pH can be varied and optimized for any particular separation problem.

With untreated fused-silica capillaries, the use of high-pH buffers generally produces fast separations due to high electroosmotic flow (EOF). At a low pH, peptides migrate primarily on the basis of their charge-to-mass characteristics and the EOF is diminished, whilst at high pH, the EOF increases. Borate, in particular, is a popular buffer in CE for a wide variety of applications, having a pH in the range of 7.5 to 10. This buffer has an inherently low conductivity (its use in CE has been reported with concentrations of 500 mM). Furthermore, it is known to complex with diol groups which facilitate analysis of sugars and glycoproteins [42].

The efficiency of this technique is, typically, much higher than the efficiency of other separation techniques, such as HPLC. Unlike HPLC, in capillary electrophoresis there is no mass transfer between phases [43].

Another important factor is that the EOF does not significantly contribute to band broadening as in pressure-driven chromatography. Capillary electrophoresis separations can have several hundred thousand theoretical plates [44] (N)- a stage in which two phases establish an equilibrium with each other, mathematically expressed as presented in the equation below:

**Equation 2 – Mathematical expression of the number of theoretical plates**

$$N=\mu V/2D_m$$

Where μ represents the apparent mobility in the separation medium and $D_m$ is the analyte's diffusion coefficient. According to this equation, the efficiency of separation is limited by diffusion and is proportional to strength of the electric field (V). In theory, unlike other types of electrophoretical assays, one could increase (dramatically, even) the voltage because the capillary has a high surface-to-volume ratio. However, in practice, the strength of the electric field is limited to several hundred volts per centimeter. If high potentials are applied, it may lead to capillary breakdown. Plus, at sufficiently high field strengths, the excessive heating becomes so strong, that radial temperature gradients can develop within the capillary. Since electrophoretic mobility of ions is generally temperature-dependent (due to both temperature-dependent ionization and solvent viscosity effects), a non-uniform temperature profile results in variation of electrophoretic mobility across the capillary, and a loss of resolution (R), which is mathematically expressed as shown below:

**Equation 3 – Mathematical expression of resolution in CE**

$$R_s= (1/4)[\triangle \mu_p N^{1/2}/(\mu_p+\mu_o)]$$

According to this equation, maximum resolution is reached when the electrophoretic and electroosmotic mobility have opposite signs and similar magnitude. In addition, one can infer that high resolution requires lower velocity and, therefore, increased analysis time[43] which can be correlated to the path taken by the analytes, meaning, the capillary's length.

Another factor that greatly influences both the resolution and efficiency of this technique is the type of transport that takes place inside the capillary- it can be either separative or dispersive:

- Separative transport arises from the interaction between the molecules and their environment, and how it affects their free energy. The separation mechanism may be based on phase equilibria, such as adsorption or ion-exchange.

- Regarding dispersive transport, or band broadening, is the total sum of processes of the dispersing zones about their gravity centers. Good examples of this are diffusion, convection and mass transfer[45].

### 1.3. The role of capillary electrophoresis in SELEX

Despite aptamers' great promise, as well as the significant effort put into their manufacture over the last two decades or so, they have been selected against only approximately 100 protein targets[46].

This slow progress is largely due to the limitations of conventional technologies used for aptamer development- SELEX.

As explained previously, SELEX involves repetitive rounds of two alternating processes- separating target-bound DNA (aptamers) from free DNA and amplification of aptamers by PCR (Figure 3).

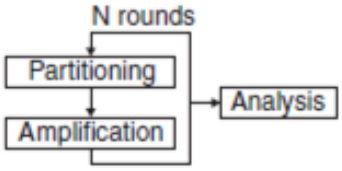


**Figure 3 - Schematic representation of aptamer selection using SELEX.**[47]

Filtration and gel-electrophoresis are two examples of non-instrumental methods of partitioning that still dominate the area[4,48,49].

As a result, SELEX based on conventional partitioning methods is not only a lengthy and resource-consuming process but, also, one that leads to DNA structures with low target-affinity or bind to the filters surface or chromatographic supports used in separation, thus compromising their viability.

Kinetic capillary electrophoresis (KCE) methods[50] have established a new methodological platform for the partitioning of aptamers.

The partitioning efficiency of KCE methods exceeds that of conventional partitioning methods, such as filtration and column chromatography, by at least two orders of magnitude[51].

As a result, KCE methods decrease the number of rounds of SELEX from 20 (required by conventional partitioning techniques)[11] to about half a dozen. Also, it has been proposed that one round might even be enough to obtain the desired aptamer, using only partitioning methods without intermediate amplification (Figure 4)- a process called non-SELEX selection of aptamers[47].

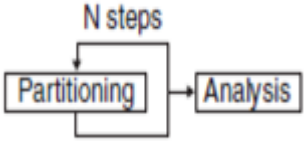


**Figure 4 - Schematic representation of non-SELEX selection of aptamers.** With this technique, the aptamers can be obtained without intermediate amplification of candidates [47]

In addition, KCE methods can be equally used for selection of aptamers and for measurements of their binding parameters, such as the equilibrium dissociation constant (Kd)[52, 53]

Also, in a recent proof-of-principle work, Krylov et al. (2006)[54] demonstrated the use of NECEEM-based non-SELEX for the selection of DNA aptamers against h-Ras protein[54], HIV-1 transcriptase[55] and selection of smart aptamers[56, 57].

Firstly used in SELEX by Bowser and co-authors under the name CE-SELEX[57], the method is perfectly applicable to targets with relatively high molecular weights, such as proteins and peptides, as it relies on electrophoretic separation (Figure 5).

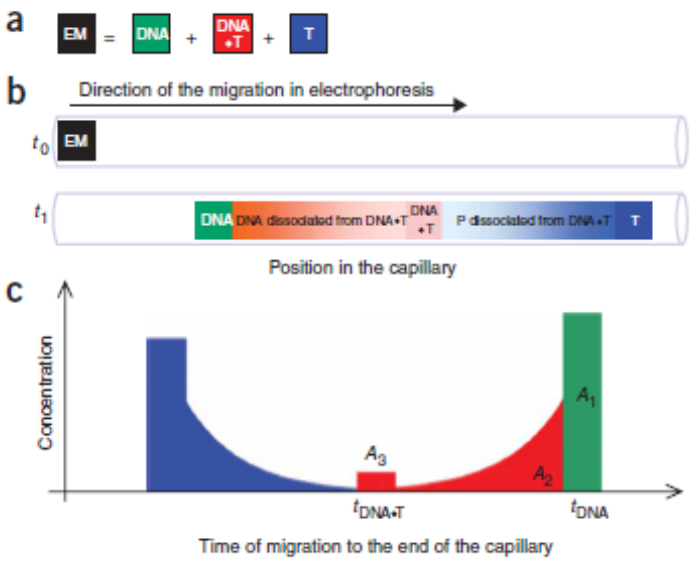


**Figure 5 - Schematic representation of NECEEM-based determination of DNA affinity to the target (T).** (a) Components of the equilibrium mixture (EM): DNA, DNA–target complex (DNA•T) and target (T). (b) NECEEM-based separation of DNA, T and DNA•T. A short plug of the EM is injected into a capillary at time $t_0$. High voltage is then applied. It is assumed that T migrates faster than DNA; DNA•T typically has an intermediate mobility. Equilibrium fractions of free DNA and T migrate as individual zones (green and blue rectangles), which do not change in time. The equilibrium fraction of DNA•T continuously dissociates during separation, leaving smears of DNA (red) and T (blue). By time $t_1$, only a fraction of DNA•T remains intact (red rectangle). (c) The parameters obtained from a single NECEEM electropherogram for the determination of $K_d$, areas $A_1$–$A_3$ and migration times of the complex (DNA•T) and free DNA (DNA) [47].

In the pre-selection steps, migration times of the target, naive DNA library and DNA–target complex (if detectable) are measured. These parameters are used to determine the time frame (or collection window) where aptamers must be collected[47].

This is the key step in separating the aptamers from the rest of the DNA, when using this technique.

Determining this window requires several tests, in order to determine the optimal conditions in which the DNA, the target and the DNA–target complex migrate inside the capillary, and it can be done in two ways: if one has a well-defined complex peak, that's where the focus goes to; if not, the collection window will go from the beginning of the target's peak to the beginning of the free-DNA's peak[47].

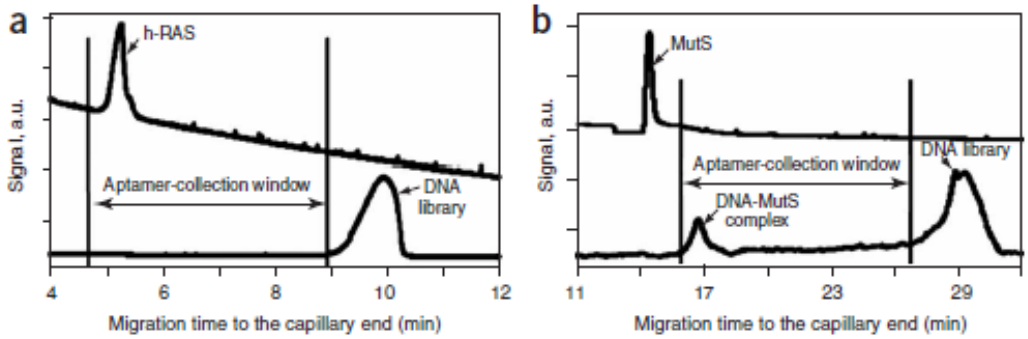


**Figure 6 – Determining an adequate aptamer-collection window.** (a) A complex of DNA with the target (h-Ras protein) is not detectable in the bulk-affinity assay. The top and bottom traces are electropherograms of h-Ras protein (UV detection at 280 nm), and the equilibrium mixture of h-Ras and naive DNA library (fluorescence detection), respectively. (b) A complex of DNA with the target (MutS protein) is detectable in a bulk-affinity assay. The top and bottom traces are electropherograms of MutS protein (UV detection at 280 nm), and the equilibrium mixture of MutS and DNA library (fluorescence detection), respectively [54].

The fractions to be collected from the output of the capillary in a time window depend of specific goals, as demonstrated in Figure 7:

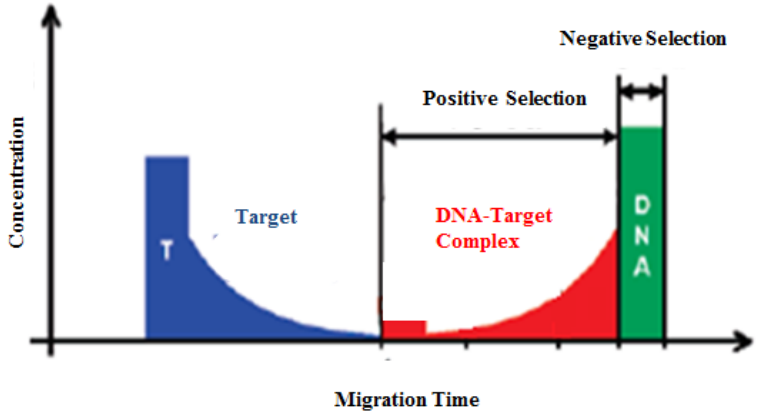


**Figure 7 – Schematics of aptamer collection: different time-frames for different fragment collections**.
Positive selection corresponds to collecting the equilibrium fraction of target-bound DNA (red), which preferably contains DNA with high affinity for the target ($K_d$ < [T]). Negative selection is the collection of the equilibrium fraction of free DNA (green), which preferably contains DNA with low affinity for the target ($K_d$ > [T]). Adapted from Berezovski, M. et al. (2006) Nonequilibrium capillary electrophoresis of equilibrium mixtures: a universal tool for development of aptamers. *Journal of the American Chemistry Society, 127,* pp 3165–3171.

In this particular case, positive selection is defined as the collection of the equilibrium part of the target-bound DNA, whereas negative selection is defined as the collection of the equilibrium part of free DNA. Each analyte has a specific window, corresponding to a specific electrophoretic pattern which, in turn, is a consequence of its own electrophoretic behavior.

Positive selection from the equilibrium mixture that contains the target can be used to select aptamers against it, being defined as defined as the collection of the equilibrium part of the

target-bound DNA. Negative selection from the equilibrium mixture that only contains the incubation buffer can be used to exclude from the library aptamers for buffer components Because the free DNA has its own electrophoretic pattern, the negative collection must be done in the same collection window as the aptamers in order to ensure that only the sequences with the most affinity are being selected.

This can be done more than once and an average of three to four rounds should be enough to obtain oligonucleotides with good affinity.

In the cloning and sequencing steps, individual sequences from the best pool are amplified by bacterial cloning and asymmetric PCR and, then, sequenced, in order to obtain the representative sequences. Those that appear to be the most repetitive are then synthesized.

In the analysis steps all the collected DNA fractions are concurrently amplified by PCR using the optimized number of PCR cycles. The strands of double stranded PCR products are separated to obtain single-stranded aptamer pools and, finally, the bulk affinities of aptamer pools to the target are measured.

Once the sequenced product is available (that is, synthesized), this step should be repeated, in order to allow an accurate measure of the aptamers' affinities.

Finally, the $K_d$ is to be obtained using the areas of the peaks obtained. This can be done with both the bulk product obtained and/or with the already synthesized aptamers, the latter giving more reliable results.

## 1.4. Bradykinin

### 1.4.1. Bradykinin and kinins

Bradykinin (Bk) is a physiologically and pharmacologically active peptide of the kinin-kallikrein system consisting of nine amino acids- Arg-Pro-Pro-Gly-Phe-Ser-Pro-Phe-Arg- and has a PI of approximately 11.31. This bioactive peptide was discovered in 1948 by Brazilian physiologists and pharmacologists working at the Instituto Biológico, in São Paulo, Brazil[58].

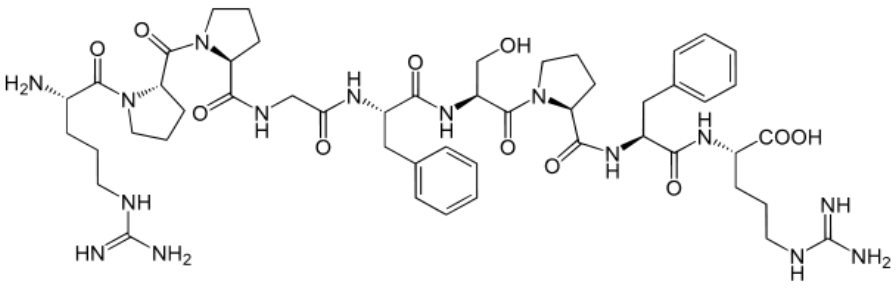


**Figure 8 – Schematic depiction of the bradykinin molecule.**

Bradykinin, lysyl-bradykinin and their des-Arg9 metabolites are mammalian peptides, collectively called kinins, involved in a number of receptor-mediated physiological actions, including inflammation and vasodilation. Bradykinin is not only important for inflammation and blood pressure regulation, but is also involved in neuromodulation and neuroprotection as well as promotion of neurogenesis[59].

A class of drugs called ACE inhibitors increase bradykinin levels (by inhibiting its degradation) further lowering blood pressure. Bradykinin works on blood vessels through the release of prostacyclin, nitric oxide, and Endothelium-Derived Hyperpolarizing Factor to promote vasodilation[60].

### 1.4.2. Bradykinin and its receptors

Bradykinin's biological activities are mediated by its specific receptors- B1 and B2[61].

The bradykinin receptors B1 and B2 (respectively, BkB1R and BkB2R or BKB1 receptor and BkB2 receptor) are G-protein coupled receptors leading to an increase in the cytosolic calcium ion concentration.

The B2 receptor is the main kinin receptor and mediates most of the known physiological action of kinins, including endothelial activation. Contrary to the B1 receptor, BkB2R is constitutively synthesized in target organs, especially blood vessels, and recognizes bradykinin and lysyl-bradykinin as its agonists[59].

Also, BkB2R is the main receptor involved in the cardiac and renal protective effects of kinins in diseases[62].

On the other hand the B1 receptor seems to be mainly synthesized only in some pathological situations, like ischemia or bacterial infection and release of bacterial toxins. Moreover, this receptor recognizes Des-arg9 kinins, produced from bradykinin and lysylbradykinin under the influence of carboxypeptidases, rather than native kinins.

Some studies point toward deleterious effects of B1 receptor activation in the setting of tissue ischemia, endotoxin induced shock or hyperglycemia. Others, however, suggest that this receptor is involved, along with B2, in the tissue protective effects of kinins during ischemia.

Interestingly, when the B2 receptor is genetically inactive, the B1 receptor is induced and can take over vascular and cardiac functions of the B2 receptor, including those involved in myocardial protection in cardiac ischemia[63].

### 1.4.3. Bradykinin and its classic therapeutic functions

Stimulation of the bradykinin B2 receptor (BkB2R or BkB2 receptor) by kinins is associated with pathophysiological as well as pronounced beneficial effects. Consequently, interference with B2 receptors by either antagonists or agonists offers promising therapeutic approaches regarding treatment of various human diseases. BkB2 receptor antagonists may prove useful for the treatment of pathological situations caused by excessively increased local kinin concentrations, such as inflammation, tissue injury and pain. Also, beneficial effects of peptide BkB2 receptor antagonists in perennial rhinitis, asthma and brain edema have already been demonstrated in clinical trials[63]. On the other hand, kinins have also been identified as potent vasodilators and organ-protective peptides. Therefore, BkB2 receptor agonists may have the potential to become valuable therapeutic tools in the treatment of cardiovascular diseases such as hypertension, myocardial hypertrophy, myocardial infarction and arrhythmias[64]. This could be achieved via the use of adequate aptamers. More specifically, these receptors' roles in pathological situations could be enhanced through the use of aptamers against bradykinin- ones that promote its pharmacological effects by preventing its degradation and, therefore, stimulate the aforementioned receptor.

Murphey LJ et al. (2001)[65] conducted a study that determined a stable metabolite of bradykinin in the systemic circulation of humans where infused bradykinin was rapidly degraded, such that no exogenous bradykinin was detected in venous plasma sampled during infusion. Bk 1-5 (Arg-Pro-Pro-Gly-Phe), the 1-to-5 amino acid fragment of bradykinin, was identified as a major stable plasma metabolite of bradykinin.

In humans, bradykinin is rapidly degraded in vivo to Bk 1-5, a stable metabolite. Measurement of this metabolite could prove to be a useful a tool to assess pathophysiologic and pharmacologic alterations in systemic bradykinin generation associated with human disease[65]. Also, it has been hypothesized that this peptide affects vasodilation, fibrinolysis and platelet aggregation in humans[66].

Interestingly, in a different study, Dr. Juerg Nussberger MD et al. (1998)[67] conducted an assay that allowed to correlate bradykinin plasma concentrations and both hereditary and acquired angioedema: bradykinin is believed to be the main mediator of symptoms in hereditary (HA) and acquired (AA) angioedema due to C1-esterase inhibitor deficiency, as well as in angioedema that complicates treatment with inhibitors of angiotensin-converting enzyme (ACE). Dr. Juerg's team was able to follow bradykinin concentrations during attacks and during remission in HA and in AA and, also, in a patient treated with an ACE-inhibitor.

22 patients with HA and 22 healthy volunteers of similar age and sex distribution were studied, as well as four patients with AA and one hypertensive patient treated with the ACE inhibitor

captopril were also studied. Among the healthy volunteers, plasma bradykinin concentration was inversely proportional to age. During acute attacks of edema, in both HA and AA, plasma bradykinin rose to values between 2 to 12 times the upper limit of normal. Infusion of C1-esterase inhibitor (the deficient factor in both HA and AA) immediately lowered bradykinin concentrations. In the patient receiving the ACE-inhibitor captopril, bradykinin concentration was very high during an acute attack of angioedema, but normal in remission after withdrawal of the drug.

This study shows that concentrations of this peptide decrease with age in healthy people. Although the differences between patients in remission and healthy controls did not reach statistical significance, there were substantial rises in plasma bradykinin during acute attacks of hereditary, acquired, or captopril-induced angioedema[67].

This study also shows that aptamers as Bk ligands could be used as diagnostic tools for pathologies to which Bk is related to. For example, a diagnostic kit could be created, using these aptamers, to measure Bk concentrations in allegedly healthy individuals of a certain age and infer about the possibility of developing angioedema. Also, these very same aptamers could be used as an alternative to ACE-inhibitors, as well as other Bk degradation inhibitors- these act on enzymes that degrade Bk, however, the aptamer would act on the target itself, therefore, making it harder to be degraded regardless of the enzyme.

However, still in regard to ACE-inhibitors, aptamers as Bk ligands also pose a viable alternative due to the fact that ACE is known to convert Aβ42 to Aβ40, the first one being a highly toxic form of beta amyloid, associated with dementia[68,69].

### 1.4.4. Bradykinin's role in neurodiferentiation and neuroregeneration

Recent studies point at functions of bradykinin in the central nervous system (CNS), including neuromodulation and neuroprotection[59]. Dr. Ulrich's team has worked previously in this subject, having reported novel functions for bradykinin in phenotype determination whether a neural progenitor cell (NPC) differentiates into a neuron or a glial cell[59].

Three *in vitro* differentiation models, P19 mouse embryonal carcinoma cells, rat NPCs, and human induced pluripotent stem cells were used to demonstrate the importance of BkB2R in neural fate and neurotransmitter receptor expression determination. As an underlying mechanism, the team has found that migration of NPCs was largely restricted when BkB2R activity was inhibited. These results were confirmed in migration assays with neurospheres obtained from BkB2R knock-out mice, which also revealed reduced migration. The group also observed a strong expression of BkB2R in the developing mouse brain, and reduced β3-tubulin

expression in BkB2R knock-out embryos. Altogether, these results indicate a novel function of Bk in the determination of cell fate in the process of neural differentiation.

In the presence of the BkB2R antagonist Hoe 140[70] during rat neurosphere differentiation, neuron-specific β3-tubulin and enolase expression was reduced together with an increase in glial protein expression, indicating that bradykinin-induced receptor activity contributes to neurogenesis. In agreement, Hoe 140 equally affected the expression levels of neural markers during neural differentiation of murine P19 and human iPS cells.

As an underlying transcriptional mechanism for neural fate determination, Hoe 140 induced up-regulation of *Notch1* and *Stat3* gene expression. Since cell viability and proliferation weren't affected during treatment, the group concluded that bradykinin-induced signaling provides a switch for neural fate determination and specification of neurotransmitter receptor expression[59].

In regard to Bk's role in neuroregeneration, Dr. Ulrich's group is, at the present moment, conducting an animal study in which the preliminary results indicate that Bk may be able to induce mobilization of endogenous stem-cells.

### 1.4.5. Other Possible Therapeutic Applications for Bradykinin

There is compelling evidence that exogenously applied or endogenously generated kinins, via stimulation of kinin-B2 receptors, activate sensory nerve terminals producing pain and hyperalgesia[71] (an increased sensitivity to pain caused by damage to nociceptors or peripheral nerves), and induce the release of proinflammatory and hyperalgesic mediators such as neuropeptides and metabolites derived from arachidonic acid pathways like leukotrienes and cytokines, which also largely contribute to their proinflammatory and nociceptive properties[72].

Bk produces short-term hyperalgesia while Des-Arg9-Bk (its active metabolite that stimulates $B_1$ receptors), causes long-term hyperalgesia. Therefore, most B2 receptor antagonists have partial agonist activity and fail to produce antinociception[73]. In the light of this information, it becomes clear that aptamers against Bk would be important tools in easing the pain of patients by inhibiting its degradation and, therefore, impairing the production of Des-Arg9-Bk whilst aptamers against this metabolite could allow for an adequate diagnostic.

Kinins also cause the formation of edema by increasing vascular permeability, plasma extravasation and contraction of smooth muscle cells, promote the migration of cells from blood to tissues and activate various tissue components. Numerous observations obtained show that decreased activity of this system may lead to cardiovascular diseases such as hypertension, cardiac failure and myocardial infarction[74]. These kinin-B2 receptor-mediated pharmacological effects are the underlying cause of the strong pro-inflammatory properties of kinins, and it is believed that excessively increased local kinin concentrations contribute significantly to

diseases like edema, rhinitis, asthma, arthritis and pain[74]. These diseases might be promising target indications for the development of kinin-B2 receptor antagonists and compounds preventing bradykinin-binding to the receptor, such as aptamers.

### 1.5. The Goal of This Project

The main goal of this project was to develop aptamers against Bk, using capillary electrophoresis as the standard technique for selection, to be used as a diagnostic tool regarding this target's concentration in the human body. Given its role in physiological actions such as inflammation and vasodilation, its role in the CNS and the role some of its metabolites' play in conditions such as hyperalgesia, fibrinolysis and platelet aggregation, it seems rather reasonable to state that these aptamers would prove to be powerful tools in the medical field.

As stated previously, even though their efficiency has been proved and considering the time that has passed since their introduction in the scientific community, there aren't that many aptamers out there. And even less have been selected using CE- a technique that has also proved to be rather useful in the field.

In order to achieve the proposed goal, a method had to be created, using the guidelines stated in this introduction, thus attaining a standardized procedure to be used again in the future, against similar targets.

# Chapter 2

## Results

The project was conducted in three parts:

1. Capillary electrophoresis assay design - migration of bradykinin, DNA pool and bradykinin-bound DNA - and determining the aptamers' $K_d$;
2. Isolation of aptamers by DNA sequencing and inferring about their structure;
3. Determining aptamers' affinity to bradykinin.

## 2.1. Capillary electrophoresis assay (migration of bradykinin, DNA pool and bradykinin-bound DNA) and Determining the $K_d$

### 2.1.1. First Selection Cycle

#### 2.1.1.1 Bradykinin Photometric Analysis

In order to provide a general oversight of the peptide, a photometric analysis was conducted, using the FlexStation 3 apparatus. At this point, the peptide and its buffer were analyzed in three different assays- one with only the buffer (blank), another with the peptide (1mM) and the buffer and a third with the peptide (in water) in a fairly high concentration (50mM). This assay allowed not only to guarantee the target's viability but, also, to determine an appropriate wavelength for analysis. The ideal wavelength would be one that showed high absorption and little to no interference.

The photometric analysis was conducted in the typical range for this kind of peptide: 200-400nm.

The results revealed major absorption at 214nm and a progressive descent along the scale, except for the blank assay, which revealed absorption exclusively at 214nm. The assay performed with the sample in a concentration of 1mM revealed absorption at 214nm as well as 260nm. When analyzing the sample at a very high concentration (50mM) and without any buffer, absorption was very high in both wavelengths- 214nm and 260nm.

a

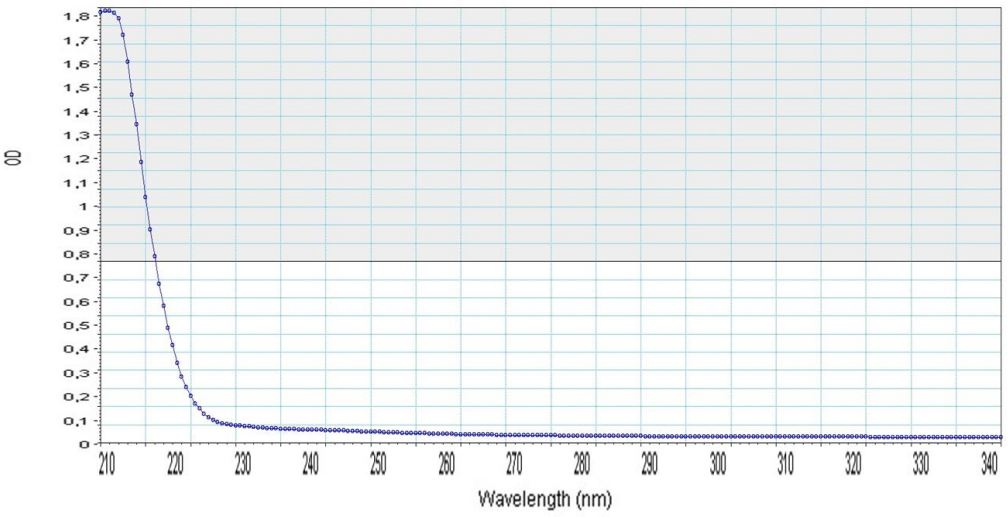


b

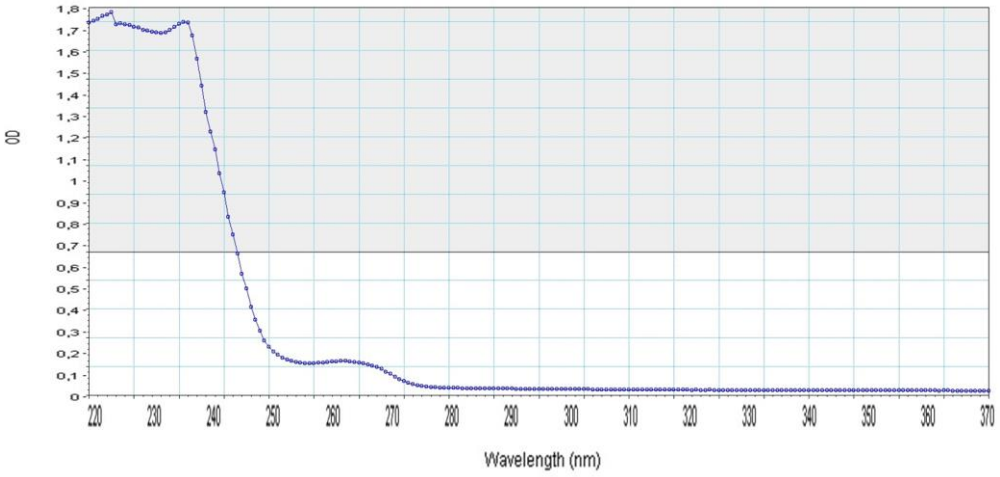


c

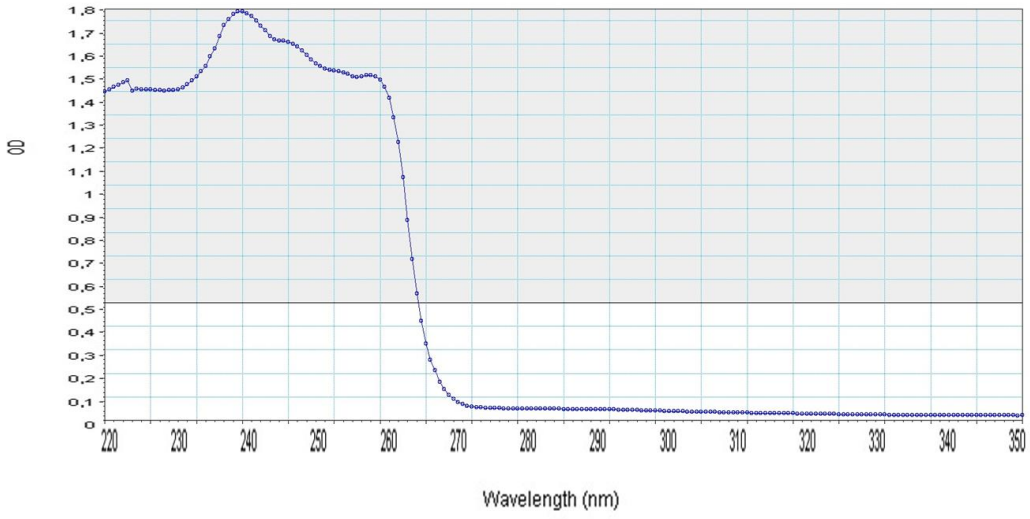


**Figure 9 – Bradykinin photometric analysis**. Results obtained when performing the spectral analysis of Bk, which were all quite similar. All showed major absorption at 214nm and a progressive descent along the scale; however, the blank assay only showed absorption at 214nm: a) Blank: Tris-HCl 10mM, $MgCl_2$ 4mM, NaCl 150mM, pH 7.4. Major absorption at 214nm. b) Bk 1mM, Tris-HCl 10mM, $MgCl_2$ 4mM, NaCl 150mM, pH 7.4. Major absorption at around 230nm. Some absorption at 260nm can also be seen. c) Bk 50mM in water. Major absorption at 214, 230 and 260nm, the latter being the one displayed.

#### 2.1.1.2. Bradykinin CE Analysis

The results to be shown from here on now were not obtained at once; rather, all required multiple attempts in different settings[a].

These attempts involved, mainly, the use of different buffers in order to establish the appropriate conditions for the ssDNA to fold and bind with the target and, more importantly, to establish an appropriate collection window.

In all assays, the areas of the peaks were calculated (automatically, in the equipment), which allowed not only to obtain the $K_d$ for each selection cycle but, also, to understand the consequences of varying the concentration of the same analyte under the same conditions and understand if there was a correlation between these two variables. The electropherograms obtained in this analysis are presented below.

The first plot shows the first run performed with the target (Figure 10 a). After that, the target was analyzed again in two different concentrations (Figure 10 b).

We have observed that, in these conditions specifically, Bk shows a detection time of around 2min and that the plot area variation is proportional to that of the concentration. Some noise was also detected.

[a] Refer to Appendix A for further information regarding previous attempts.

a

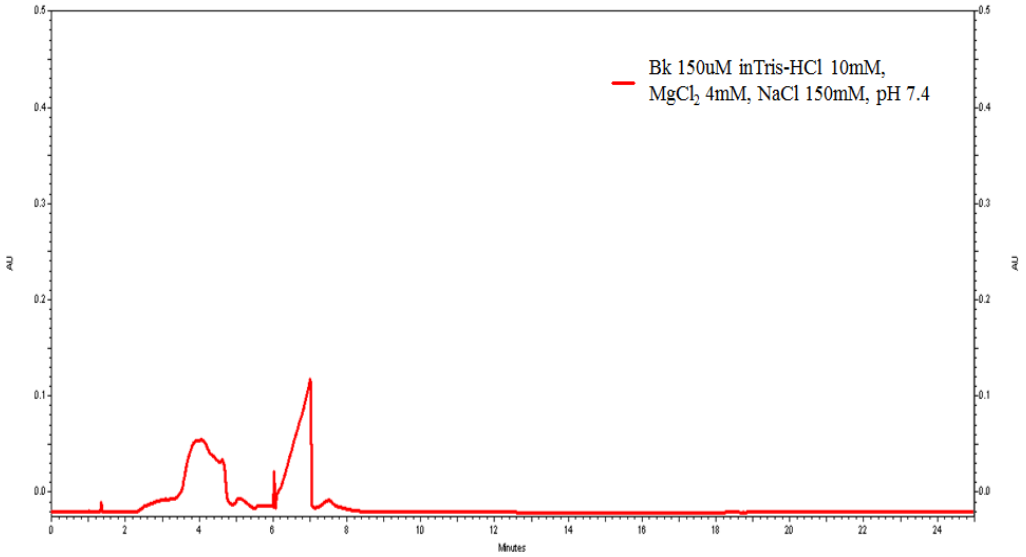


b

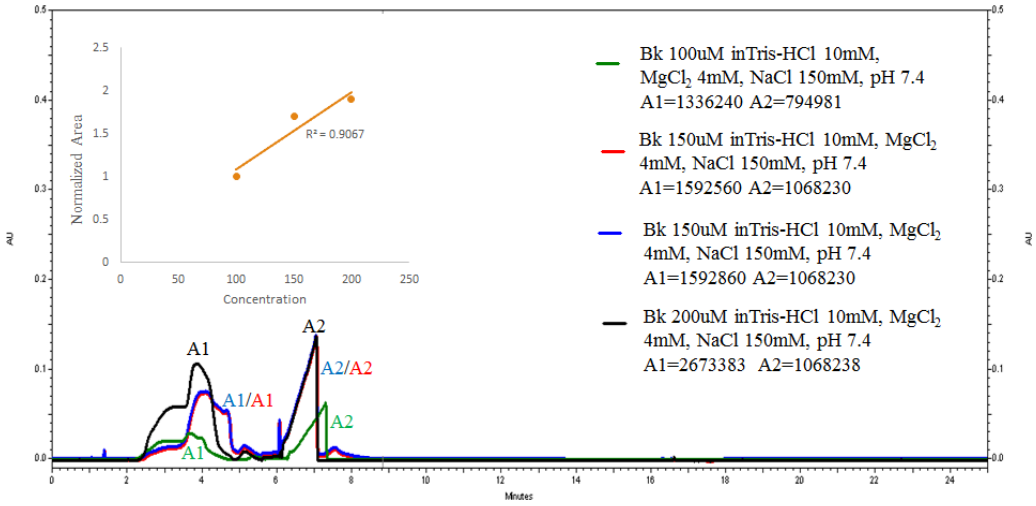


**Figure 10 – Bradykinin analysis by capillary electrophoresis**. a) First run with Bk: Bk 150uM in Tris-HCl 10mM, $MgCl_2$ 4mM, NaCl 150mM, pH 7.4. Capillary: 60cm total length, 75µm ID, 375µm OD. Separation buffer: borate 25mM, pH 9.3. 214nm wavelength. Capillary temperature: 25ºC b) Overlay of the first run with three others. Same conditions with varying Bk concentrations. The areas, obtained with the equipment, have been normalized in order to analyze the linearity between the peaks and the concentration- an average value was calculated using all values for each observable peak.

Interestingly, there's a peak on the far right that does not quite seem to agree with what was expected.

In order to understand what it might be, a blank assay was performed (Figure 11 a), revealing that that peak can be attributed to the electroosmotic flow (EOF). After that, in order to guarantee that the conclusion is reliable, the results obtained with bradykinin were compared to those obtained with CD73 (Figure 11 b) - a protein that converts AMP to adenosine and phosphate, which, in turn, activates specific receptors on the membranes of the immune system's cells - which was being studied by Dr. Arquimedes Cheffer who intends to develop

aptamers against it. We have observed that that same peak is also present, which means that, indeed, there is EOF to be considered in these assays.

a

b

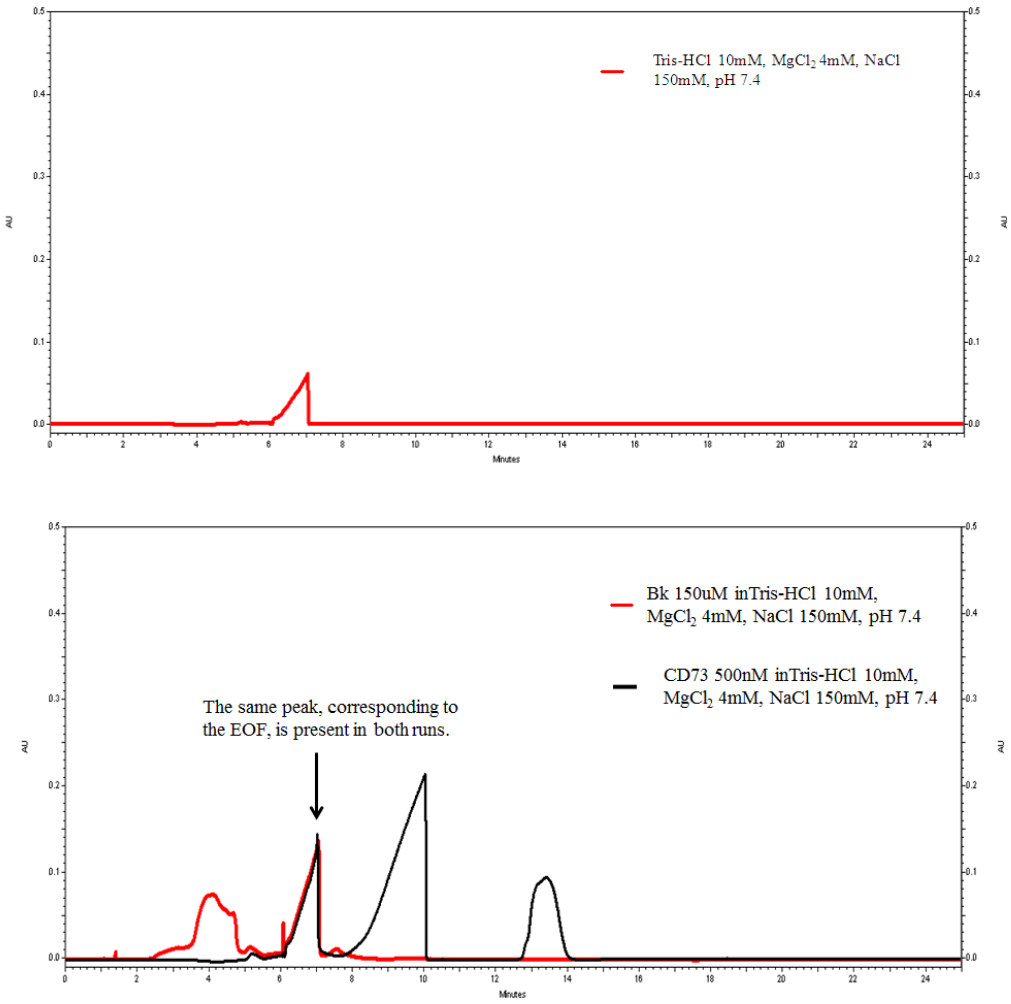


**Figure 11 – Buffer interference**. a) Blank assay: Tris-HCl 10mM, $MgCl_2$ 4mM, NaCl 150mM, pH 7.4. Capillary: 60cm total length, 75um ID, 375um OD, 214nm wavelength. b) Bk 150uM overlaid with CD73 500nM and CD73 500nM. Separation buffer: borate 25mM, pH 9.3. The overlaid peaks are quite noticeable, representing the interaction between the buffer and the sample buffer in both cases.

### 2.1.1.3. DNA and DNA-Target Complex

In regard to the original DNA pool (a random DNA pool purchased from Life Technologies, containing 70bp), it was amplified using a standard PCR procedure, so that more product could be used and, then, submitted to a denaturizing gel electrophoresis assay, since the DNA is required to be single stranded.

The result obtained was quite satisfactory, as it allowed the experiment to continue.

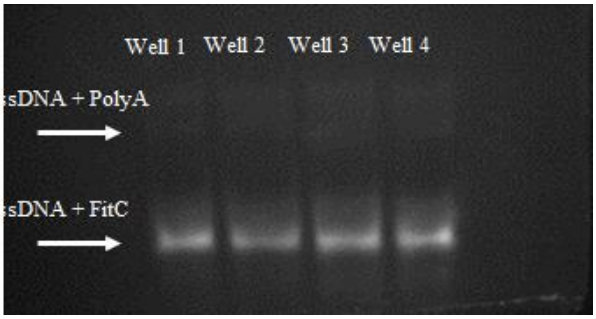


**Figure 12 - Denaturizing PAGE after template amplification**. All four wells contain the original DNA library. The arrows point to both strands after separation. The one on top contains the primer marked with PolyA, whereas the one on the bottom contains the primer marked with FitC.

After amplification and strand separation, the DNA was submitted to the standardized folding procedure[b].

After this, the DNA pool was analyzed with the CE apparatus, using the same method as described before for the peptide with the LIF detector mounted. Again, multiple runs were performed, using different DNA concentrations- 100, 150 and 200nM- all in the same buffer- tris-HCl 10mM, $MgCl_2$ 4mM, NaCl 150mM, pH 7.4. As with other plots presented here, varying the concentration allows to infer about the linearity of the assays performed and peak identification. The ssDNA presented an average migration time of around 10min, and considerable fluorescence, even with a concentration of 100nM (Figure 13). As seen when analyzing bradykinin, the area variation of the plots is proportional to that of the analyte's concentration.

[b] Protocol described in chapter 4, section 4.6.

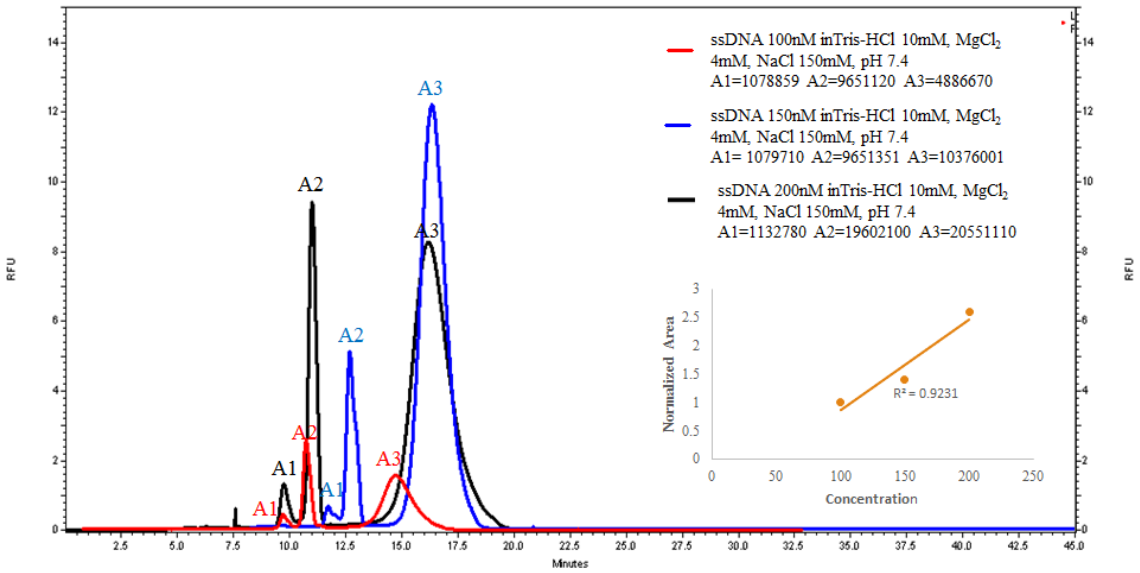


**Figure 13 – First three runs with the original ssDNA pool.** Three different concentrations were used- 100nM, 150nM and 200nM- all in tris-HCl 10mM, $MgCl_2$ 4mM, NaCl 150mM, pH 7.4. Capillary: 60cm total length, 75µm ID, 375µm OD. Separation buffer: borate 25mM, pH 9.3. The areas, obtained with the equipment, have been normalized in order to analyze the linearity between the peaks and the concentration- an average value was calculated using all values for each observable peak.

After this, a new sample of the same ssDNA was appropriately prepared and incubated with the target, in order to be analyzed. This assay was performed three times, under the same conditions as the ssDNA, revealing fluorescence values in the same order. The complex was detected at around 7.5min.

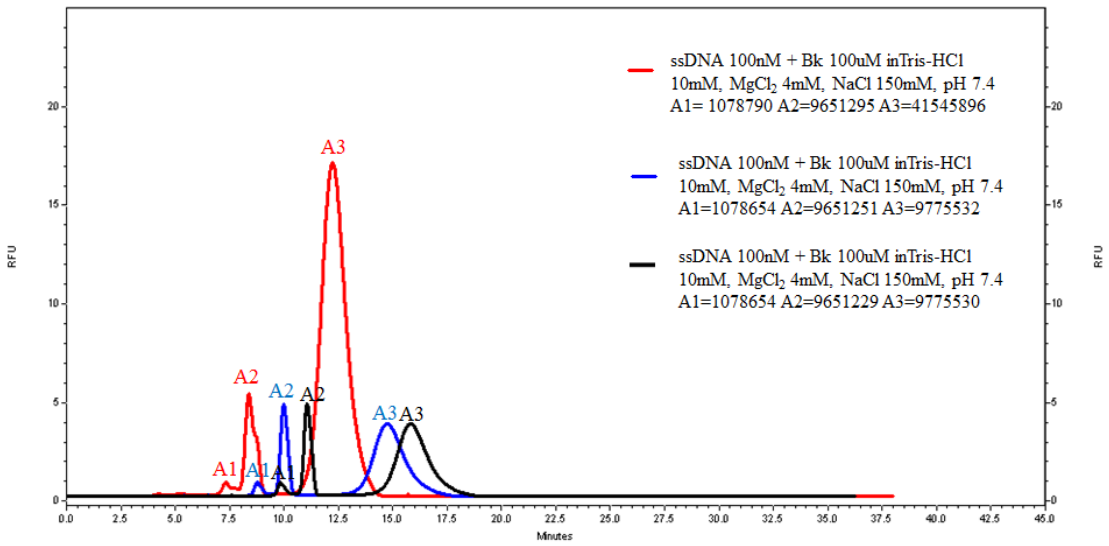


**Figure 14 – Three overlaid runs of the DNA-target complex.** All samples in tris-HCl 10mM, $MgCl_2$ 4mM, NaCl 150mM, pH 7.4. Capillary: 60cm total length, 75µm ID, 375µm OD. Separation buffer: borate 25mM, pH 9.3. Despite the concentration being the same in all runs, there was a significant area variation in one of them. It is possible that the fluorophore burned out or that the DNA adopted a structure that induced quenching.

### 2.1.1.4. Defining the Collection window

Once these assays were concluded, one had to define an appropriate collection window. In order to do this, one has to consider both the total length of the capillary ($L_{total}$) and the length from the injection point to the detection window ($L_{detector}$) have to be taken into consideration[47]. These values allowed us to determinate the correction factor, which will, then, be multiplied by the starting and ending points of the window, on the horizontal axis. This is crucial, since it allowed us to understand at what point the sample we're observing on screen is ejected to the output vial. In other words, it is the actual time it takes for the sample to run through the whole capillary.

Since the ssDNA-target complex did not present a specific peak, the collection window was defined considering the detection times of the target and the ssDNA. More specifically, it begins when the target starts to show up and stops right before the ssDNA starts to show up, thus guaranteeing that any genetic material collected corresponds to the aptamers.

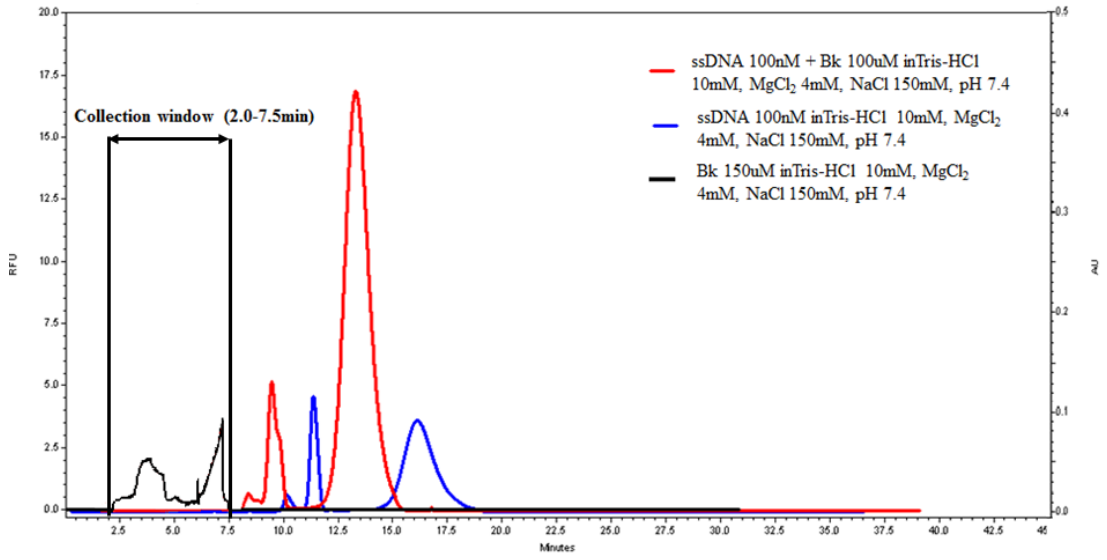


**Figure 15 – Schematic depiction of the collection window used in the first selection round.** The window was defined considering that the complex peak is quite similar to that of the ssDNa[47]. Two collections have been made- negative and positive. The plots presented have been showed previously.

The fraction collection was performed 10 times for both the positive and negative controls[c]. Both DNA pools were then submitted to 15 cycles of PCR, in order to allow adequate manipulation.

The $K_d$[47] obtained for this cycle was 73µM[d].

[c] Refer to Figure 7 - chapter 1, section 1.5 - for further reference on both positive and negative controls regarding this technique.

### 2.1.2. Second Selection Cycle

#### 2.1.2.1. Preparing the ssDNA

The start of a new selection cycle resembles that of the previous one- it begins with a standard PCR reaction, strand separation and CE analysis, ending with yet another DNA fraction collection.

Both controls were submitted to 15 cycles of PCR (the lab's standard procedure)[e], in order to allow adequate manipulation. After this, a PAGE assay was performed[f], in order to confirm the results. Five wells were used in total, containing a blank assay (water as template), the negative control (negative collection), a positive control (the original library), the template (positive collection) and a 100bp ladder as marker. The results revealed that the collection was a success, since no unspecified genetic material was amplified (meaning it had not been collected) whereas the aptamers had. Also, there was no primer self-replication. ***Figure 16***

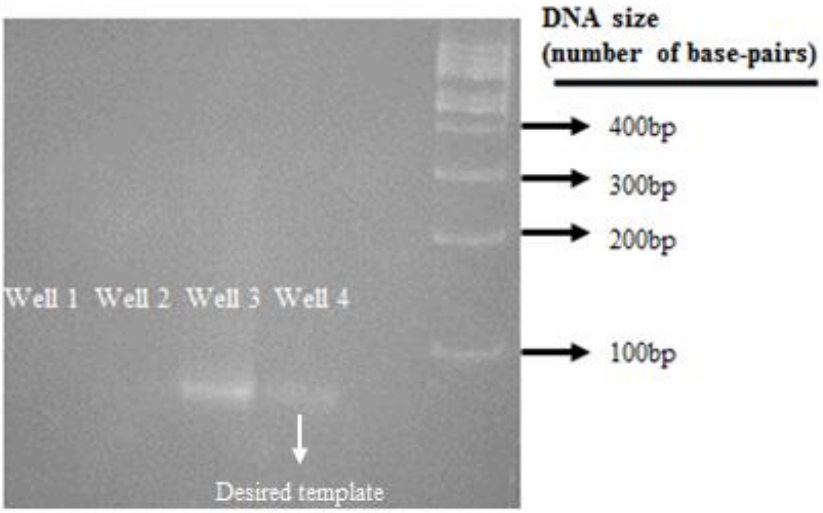


**Figure 16 – Standard PAGE assay for evaluating the success of the collection process.** From left to right (well 1 through well 4): blank, negative collection, positive control and positive collection. The 100bp ladder is on the far right. Well 1 indicates that there was no amplification of non-specified template, well 2 indicates that the collection window is adequate and that no free ssDNA is being collected. The DNA ladder is on the far right, along with the base-pairs sizes for each band.

After the first set of cycles, a series of PCRs with a different number of cycles was done. The assay was performed using the protocol described earlier. In this case, a total of 7 wells was used- 100bp ladder in the first and the samples, with the appropriate template, in all the others.

[d] Refer to chapter 4, section 4.8, for further reference on how this value was obtained.
[e] Protocol described in chapter 4, section 4.2.
[f] Protocol described in chapter 4, section 4.3.

Each sample was subjected to a different number of cycles- 2, 5, 8, 11, 13, 15. The results obtained revealed that 8 cycles was ideal. This was done to guarantee maximum amplification of the desired template and no amplification of non-specific genetic material, which is crucial to guarantee that the oligonucleotide sequences remain unaltered.

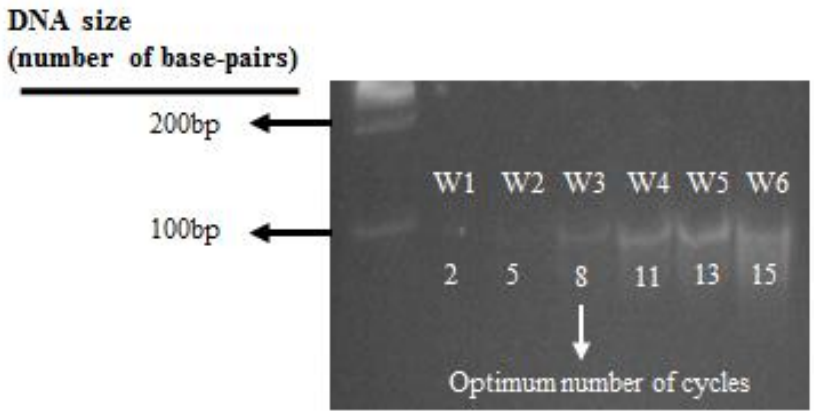


**Figure 17 - PCR series with varying number of cycles**. Six reactions with varying number of cycles were done- 2, 5, 8, 11, 13 and 15- in all 6 wells (W1 through W6, respectively). All wells contained the same original template, varying only in amount of amplified product, due to the different number of PCR cycles. Only the last 4 wells showed signs of amplification. The far left well contains the 100bp ladder.

After establishing an adequate number of cycles, a new PCR was made[g] (using that number of cycles) with enough template for thirty reactions, yielding a total of 3ml. After this, the aforementioned solution's DNA was precipitated and underwent a strand separation procedure[h]. After that, the typical DNA extraction protocol was applied[i]. Once the ssDNA had been extracted and appropriately diluted in water, the new selection round began.

### 2.1.2.2. Re-Analyzing the Target

First, the target was analyzed (as it had been previously) in the CE apparatus, with a 30cm capillary and, because its length was reduced in half, the same happened to the voltage used in the particle separation- a total of 9kV were used. Both the separation and sample buffers, however, remained the same

In these specific conditions, the target's detection time was and bradykinin was detectable almost from the start (0min). In regard to the area variations, the proportion between these and

[g] Protocol described in chapter 4, section 4.2
[h] Protocol described in chapter 4, section 4.4
[i] Protocol described in chapter 4, section 4.5

the concentration remained unaltered. The peaks' shapes were considerably different, which can be attributed to the capillary's length being reduced.

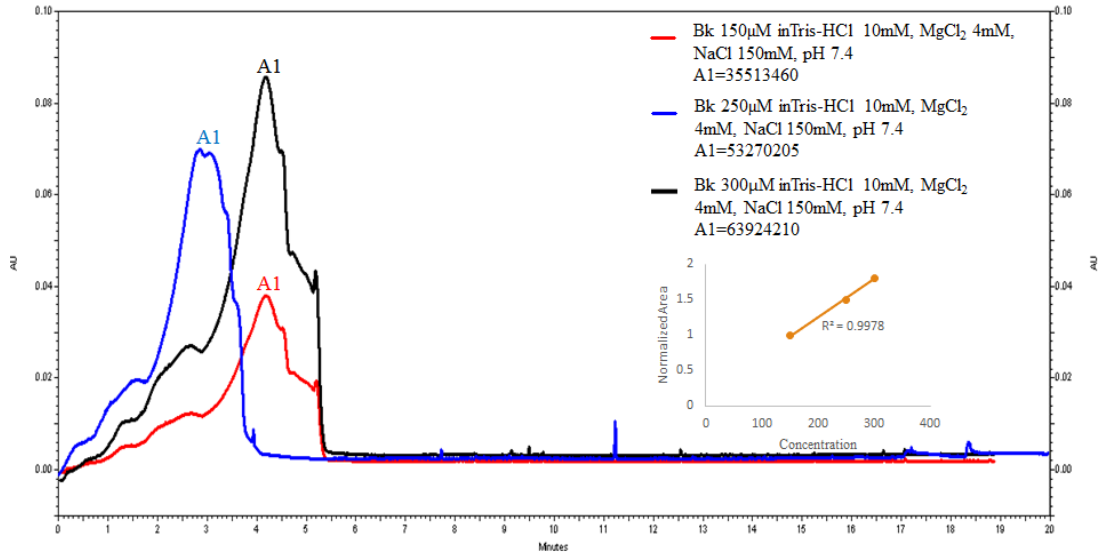


**Figure 18 - Bk analysis or the second cycle in different concentrations.** Three concentrations were used- 150, 200 and 300µM- in tris-HCl 10mM, $MgCl_2$ 4mM, NaCl 150mM, pH 7.4. Capillary: 30cm total length, 75um ID, 375um OD, 214nm wavelength. Separation buffer: borate 25mM, pH 9.3. The lack of resolution can be attributed to the short length of the capillary which, in itself, demanded a re-adjustment of the scale used during the data processing. The areas have been normalized- an average value was calculated using all value for each observable peak. Then, all values obtained were divided by the smallest one.

### 2.1.2.3. Analyzing the Selected Oligonucleotides

As before, after the analyzing the target, the ssDNA that resulted from the previous selection cycle was analyzed.

As with bradykinin, the detection time was diminished by approximately 2min, thus, the ssDNA was visible at around 8min. The direct correlation between the variation of the plots' area and that of the analyte's concentration was slightly diminished in this case. Regarding the peaks' shapes, however, contrary to what had been seen when analyzing the target, the variation was less significant.

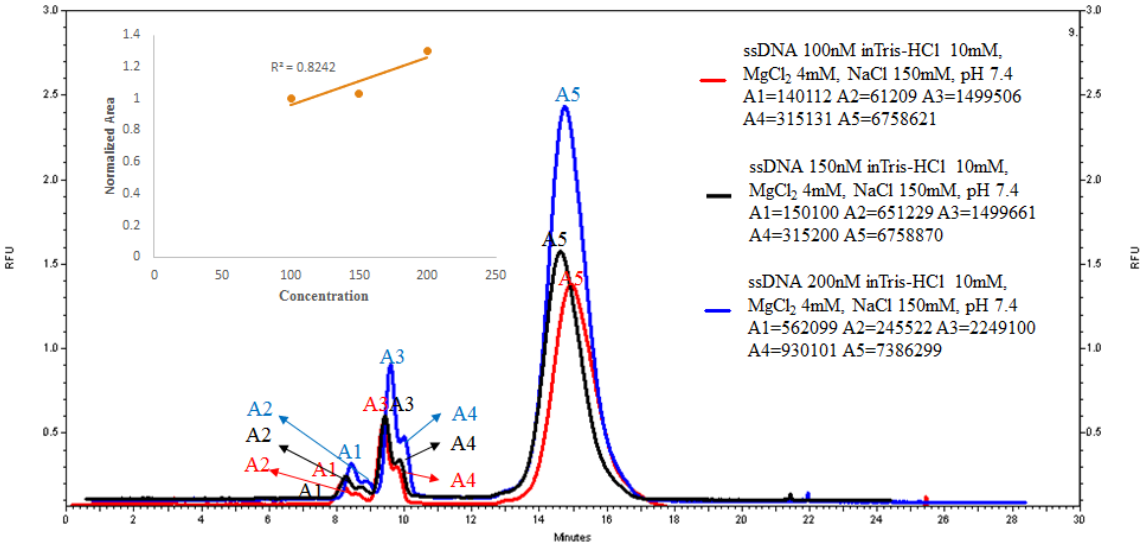


**Figure 19 - Three different runs for three different concentrations**. Three different concentrations of the oligonucleotide sequences selected in the previous cycle were used- 100, 150 and 200nM- all in tris-HCl 10mM, $MgCl_2$ 4mM, NaCl 150mM, pH 7.4. Capillary: 30cm total length, 75µm ID, 375µm OD. Separation buffer: borate 25mM, pH 9.3.The areas have been normalized- an average value was calculated using all values for each observable peak. Then, all values obtained were divided by the smallest one.

### 2.1.2.4. Analyzing the New DNA-Target Complex

After that, the DNA was folded[j] and incubated with the target. Three runs were made, with varying concentrations of target and ssDNA. In these conditions, the detection time of the aptamer-target complex was of approximately 10min and, as with the previous cycle, the peaks' shapes were pretty similar to that of the ssDNA, as were the fluorescence levels (when considering the same concentrations of ssDNA and target).

[j] Protocol described in chapter 4, section 4.6.

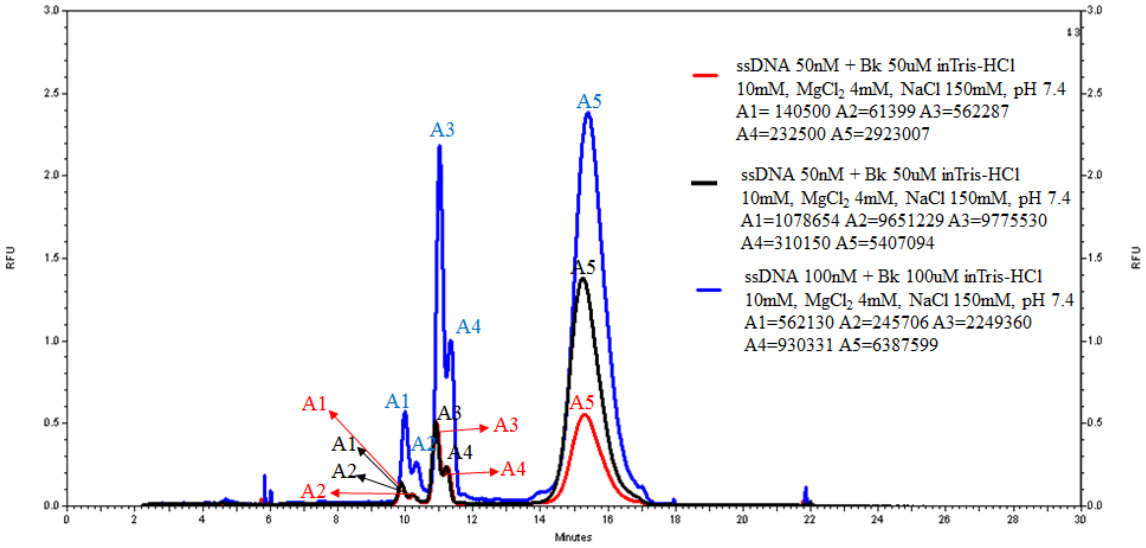


**Figure 20 - Fig. – Three different runs of the new aptamer-target complex.** All samples in tris-HCl 10mM, $MgCl_2$ 4mM, NaCl 150mM, pH 7.4. Capillary: 30cm total length, 75µm ID, 375µm OD. Separation buffer: borate 25mM, pH 9.3). The values marked A1 through A5 represent the areas of each observable peak, from left to right. The areas, obtained with the equipment, have been normalized in order to analyze the linearity between the peaks and the concentration- an average value was calculated using all values for each observable peak.

### 2.1.2.5. Defining the New Collection Window

The new collection window was defined in a similar way to that of the first (as depicted in Figure 21), which means that it started in the same moment that the target shows up (0min, in this particular case) and stops right before the ssDNA starts to show up (7min).

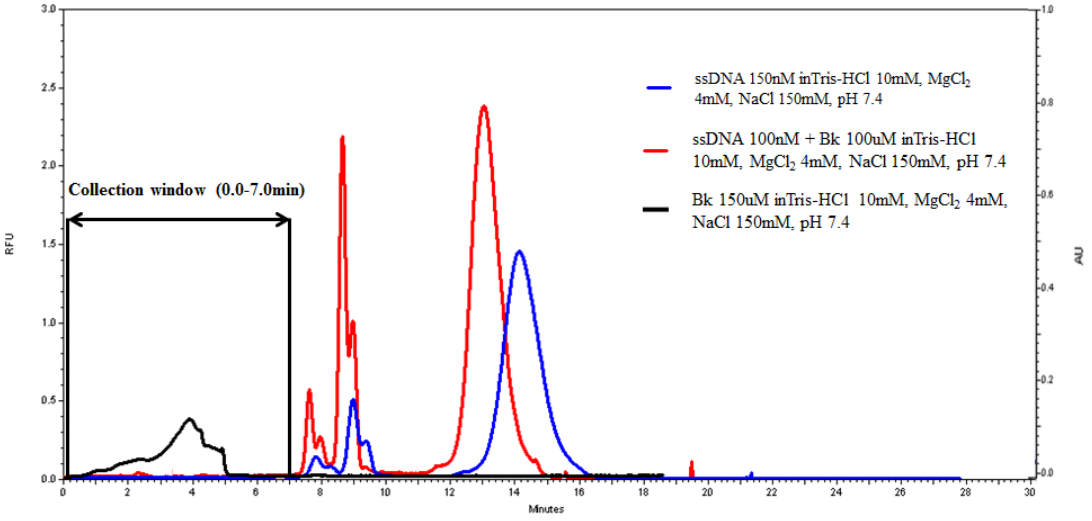


**Figure 21 - Schematic representation of the collection window used in the second selection cycle**. Two collections were made- positive and negative- as explained in pages 10-12. The plots presented have been shown previously.

After this, the product obtained was submitted to a 15 cycle PCR reaction[k]. As was done in the previous cycle, in order to confirm that the collection window is adequate, a simple PAGE[l] assay was done. Figure 22 shows the results obtained: the first well, which contained all reagents necessary for amplification except for the template, reveals that there was no amplification of any kind (including primer self-replication); the second well, which contained the negative collection and had no amplification reveals that that collection contained no oligonucleotides whatsoever; the last two wells contained, respectively, a positive control and the positive collection, both showing signs of amplification, thus indicating that the procedure was a success.

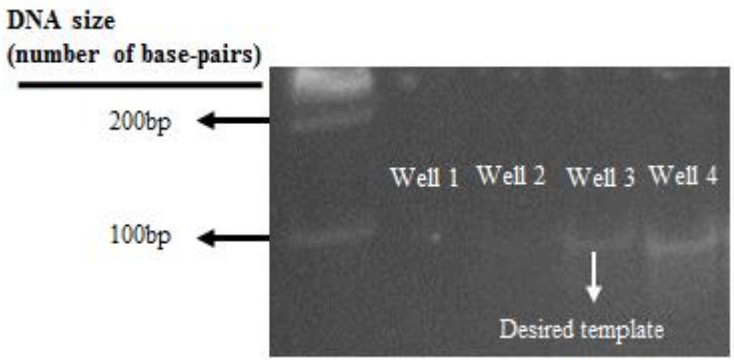


**Figure 22- Standard PAGE assay for evaluating the success of the collection process**. From left to right: blank, negative collection, positive collection, positive control. The first well indicates that there was no amplification of non-specified template. The second one indicates that the collection window is adequate and that no free ssDNA is being collected (which is why the well is empty). The third well contains the collected aptamers and the fourth contains a positive control.

As before, another series of PCRs[m] were performed, in order to evaluate the optimum number of cycles that allowed aptamer amplification with no unspecified product. 4 reactions were made, with 3, 5, 8 and 11 cycles. When performing a simple PAGE assay[n], we verified that 8 cycles was the optimum number.

[k] Protocol described in chapter 4, section 4.2.
[l] Protocol described in chapter 4, section 4.3.
[m] Protocol described in chapter 4, section 4.2.
[n] Protocol described in chapter 4, section 4.3.

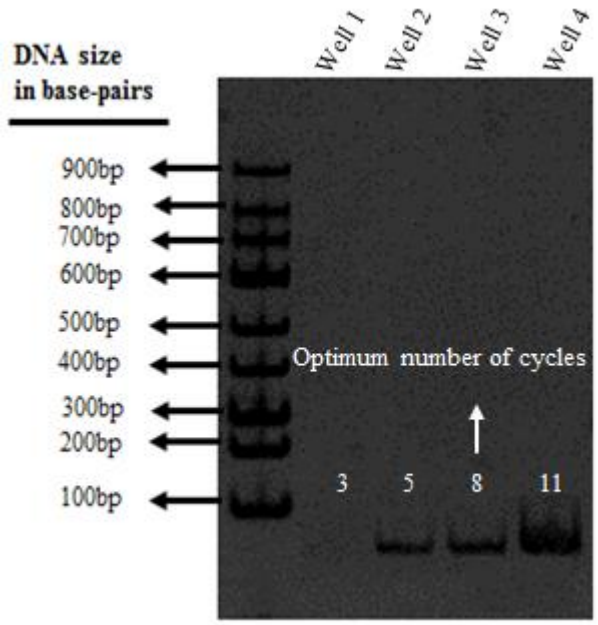


**Figure 23 – PCR series with varying number of cycles**. Series of PCR assays using different number of cyckes- 3, 5, 8 and 11- in all 4 wells. All wells contained the same original template, varying only in amount of amplified product, due to the different number of PCR cycles to which they were submitted. The far-left well contains the 100bp ladder.

After this, a considerable amount of this product was subjected to this very same number of cycles, in the exact same conditions. The material obtained was then used in parts 2.2 and 2.3 of this project. The $K_d$[o] obtained in this cycle was 54µM[p].

## 2.2. Aptamer Sequencing and Structure Analysis

100 colonies were used to sequence the aptamers[q], yielding 80 valid sequences. After manual selection, in which a great deal of sequences were discarded due to lack of similarities between them and/or gaps, the selected ones were grouped, considering their repetitive motifs. This analysis was done using the MEME-suite software (developed and maintained by the University of Queensland, the University of Washington and the National Center for Research Resources, among a few others).

A total of 6 motifs were found, present in 16 sequences. Each motif was assigned to a group, which may contain anywhere from 2 to 4 sequences. Sequences 1.2 and 1.3 both have 2 motifs and sequence 2.1 has 3 motifs. Table 1 depicts these results.

[o] Refer to Figure 7- chapter 1, section 1.5- for further reference on both positive and negative controls regarding this technique.
[p] Refer to chapter 4, section 4.8, for further reference on how this value was obtained.
[q] Protocol described in chapter 4, section 4.9

**Table 1 – Selected sequences grouped according to the repetitive motifs**. Conserved regions within individual classes of aptamers are underlined. All sequences start and end with the primers GGGAGACAAGAATAAGCG and AGGAGGCTCACAACAGG, respectively. The sequences in bold are present in more than one group (e.g. 3.1 is the same as 1.2, 3.4 is the same as 1.3, 5.1 is the same as 4.2 and 2.1). Each motif defines a specific group. Sequences are numbered considering the group they correspond to and the order by which they were depicted.

| Group Number and Motif | Sequences | Sequence Number |
|---|---|---|
| 1 TTGAGCCCGGG | 5' GCACGCGCCCGCACCACGCCTTTGAGCCCGGGGA 3' | 1.1 |
| | **5' GCACGCGACGGTCCGCACGCGCTTGAGCCCGGGA 3'** | **1.2** |
| | **5' GCACAGGACGGGCCGCACCGCTTGAGCCCGGGGA 3'** | **1.3** |
| 2 AAAGGGA | **5' CCACCACGAGGTGCTACCTTAGCGGCAAAGGGAA 3'** | 2.1 |
| | 5' CCACCACGAGGTGTACTAGCGGCAAAGGGAAAGG 3' | 2.2 |
| | 5' ACAATTGTGTGACGAGGTAGCAAAGGGAATCTGA 3' | 2.3 |
| 3 ACGGGCCGGA | **5' GCACGCGACGGGCCGGACGCGCTTGAGCCCGAGA 3'** | **3.1** |
| | 5' GGCGGACGGGCCGGACGTGACGTGAGCGCGCGAA 3' | 3.2 |
| | 5' GGGCAGCGAGCAAGAACGGGCCGGACATCGCTGC 3' | 3.3 |
| | **5' GCACAGGACGGGCCGGACCGCTTGAGCCCGGGGA 3'** | **3.4** |
| 4 TGCTACCTT | 5' GCTTTAAGACGATGCTACCTTGATTTGCTTTATC 3' | 4.1 |
| | **5' CCACCACGAGGTGCTACCTTAGCGGCAAAGGGAA 3'** | **4.2** |
| 5 ACCACGAGG | **5' CCACCACGAGGTGCTACCTTAGCGGCAAAGGGAA 3'** | **5.1** |
| | 5' CCACCACGAGGTGTACTAGCGGCAAAGGGAAAGG 3' | 5.2 |
| 6 ACTGCT | 5' CCAGCAGACGGTACTGCTCGCACTGGACGTGCAC 3' | 6.1 |
| | 5' GTGCGTCCCGTACTGCTAGGCCTAAGCGTGTGCG 3' | 6.2 |

These sequences were, then, analyzed using the Mfold software (designed by the RNA Institute, College of Arts and Sciences, State University of New York, Albany), thus providing a prediction of the structural arrangement of the aptamers. This step provided information regarding the aptamers' stability (the average ΔG for all structures was around -20) as well as identification of the site(s) where the aptamers interact with the target- the site(s) where the motif(s) lie within the structure. Sequences that have similar motifs in composition share that similarity in the structure, meaning that motifs that are present in more than one sequence are so also in analogous positions, as depicted in Figure 24.

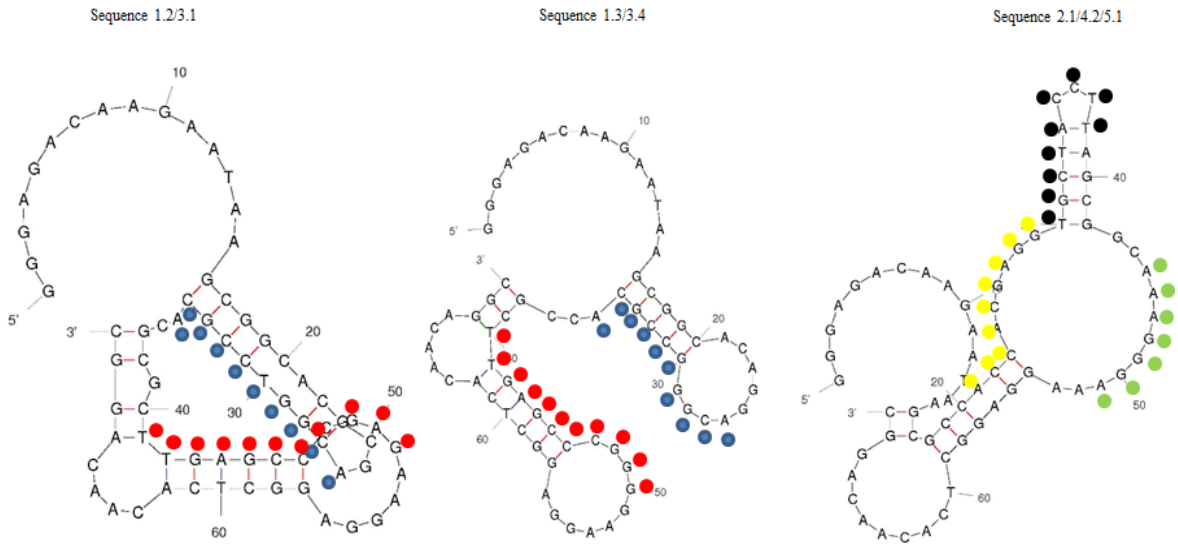


**Figure 24 – Representation of the secondary structures of the sequences 1.2/3.1, 1.3/3.4 and 2.1/4.2/5.1.** The colored dots mark the motifs that define each group- blue for group 1, green for group 2, red for group 3, black for group 4 and yellow for group 5. The groups are characterized by the motifs that define them, as stated above. The sequence names are attributed according to the group(s) that they fit into- the first digit represents the group and the second the order in which the sequence is depicted. If a sequence fits in more than one group (meaning it has more than one motif), its name will be characterized by more than one set of digits, separated by "/" (*ex:* sequence 1.2/3.1 is the second sequence in group 1 and the first in group 3).

### 2.2.1. Aptamer Structures and Motifs

The following is a depiction of the most relevant aptamer structures obtained with the Mfold software (designed by the RNA Institute, College of Arts and Sciences, State University of New York, Albany).

#### 2.2.1.1. Aptamer Groups 1 and 3

Groups 1 and 3 have, respectively, the motifs TTGAGCCCGGG (marked in red) and ACGGGCCGGA (marked in blue). Apart from structure 3.3, all the structures are non-linear. Sequences 1.2/3.1 and 1.3/3.4 have two motifs, both in positions that indicate a possible lock and key-type of interaction between the aptamer and the target.

As far as the alignment goes (see Table 1), both these groups present fairly similar sequences.

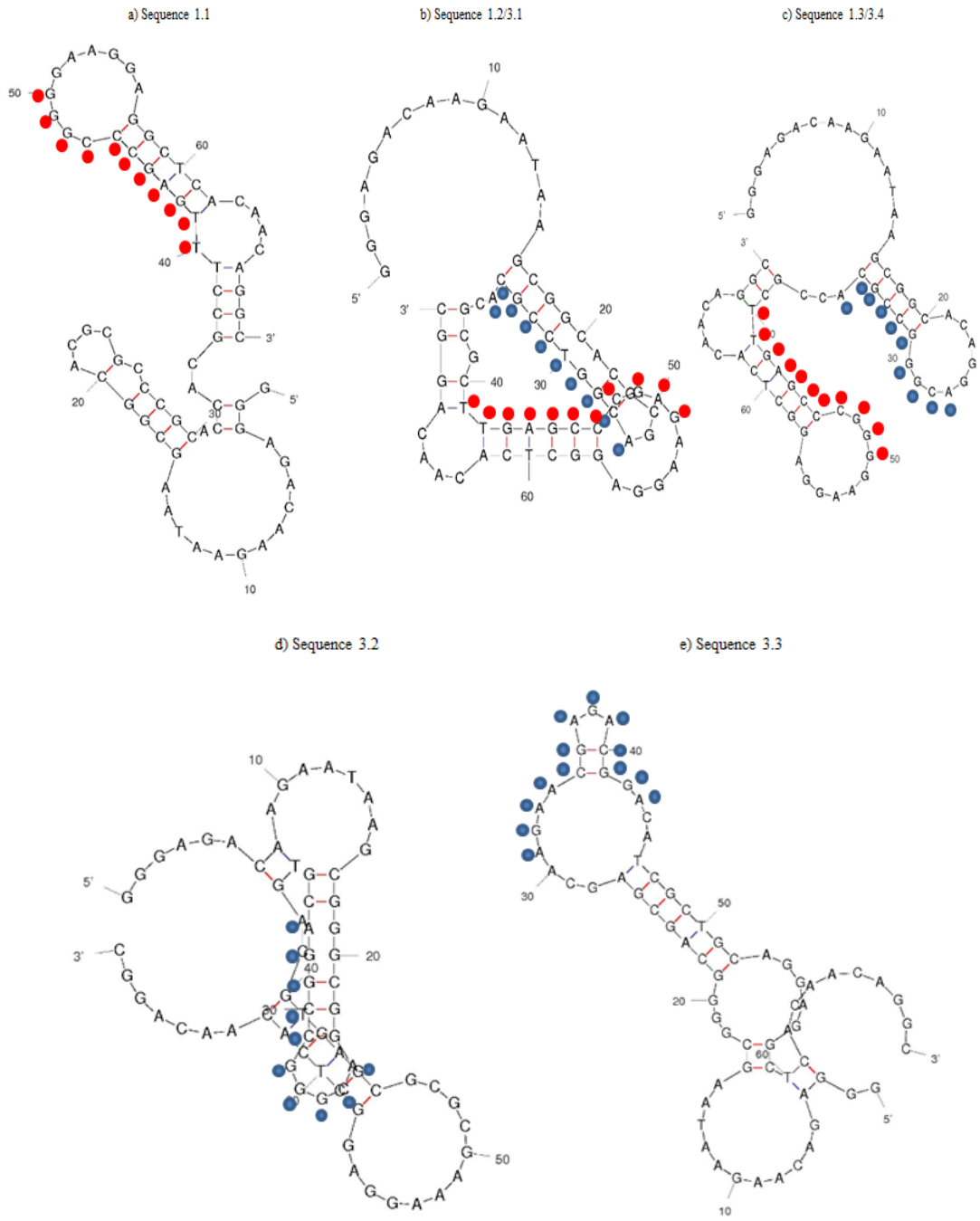


**Figure 25- Aptamers of groups 1 and 3**. Figures a through e depict the structures in groups 1 and 3. The colored dots mark the motifs that define each group- blue for group 1 and red for group 3. The groups are characterized by the motifs that define them, as stated above. The sequence names are attributed according to the group(s) that they fit into- the first digit represents the group and the second the order in which the sequence is depicted. If a sequence fits in more than one group (meaning it has more than one motif), its name will be characterized by more than one set of digits, separated by "/".

### 2.2.1.2. Aptamer Groups 2, 4 and 5

Groups 2, 4 and 5 have, respectively, the sequences AAAGGGA (marked in green), TGCTACCTT (marked in black) and ACCACGAGG (marked in yellow). Sequence 2.1/4.2/5.1 fits in all 3 groups, whereas sequences 2.3 and 4.1 only fit in groups 2 and 4, respectively. Albeit not as evident, it is possible that the lock and key-type of interaction is also present in these groups.

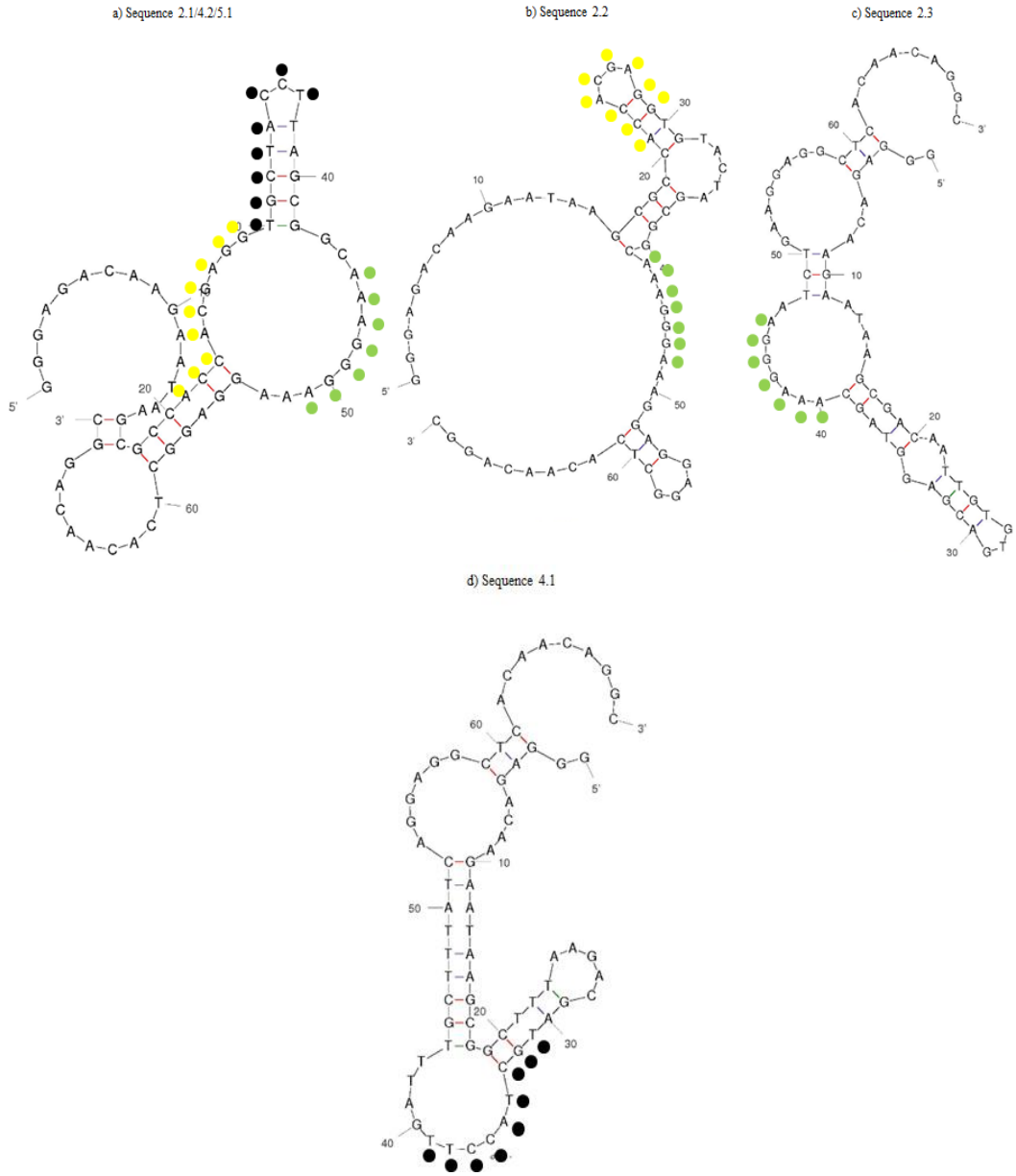


**Figure 26- Aptamers of groups 2, 4 and 5**. Figures a) through d) depict the structures in groups 2, 4 and 5. The colored dots mark the motifs that define each group- green for group 2, black for group 4 and yellow for group 5. The groups are characterized by the motifs that define them, as stated above. The sequence names are attributed according to the group(s) that they fit into- the first digit represents the group and the second the order in which the sequence is depicted. If a sequence fits in more than one group (meaning it has more than one motif), its name will be characterized by more than one set of digits, separated by "/".

### 2.2.1.3. Aptamer Group 6

Group 6 corresponds to the sequence ACTGCT (marked in brown).

Only two sequences fit in this group (sequences 6.1 and 6.2).

Similarly to group 3, it is constituted by 6 bases which, as before, do not show such an evident lock and key-type of interacting system.

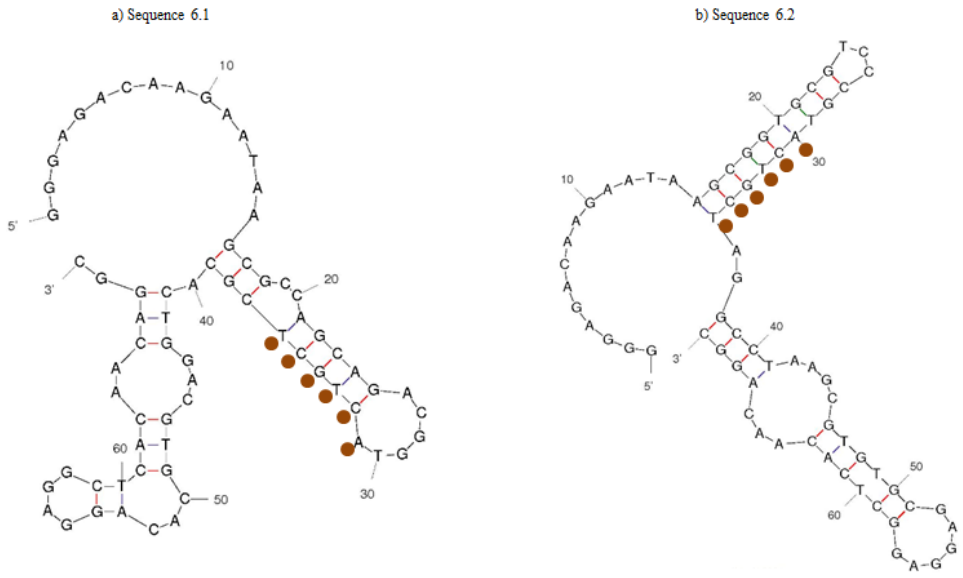


**Figure 27- Aptamers of group 6**. Figures a) and b) depict the structures in group 6. The colored dots mark the motifs that define each group. The groups are characterized by the motifs that define them, as stated above. The sequence names are attributed according to the group(s) that they fit into- the first digit represents the group and the second the order in which the sequence is depicted. If a sequence fits in more than one group (meaning it has more than one motif), its name will be characterized by more than one set of digits, separated by "/".

## 2.3. Aptamer Affinity Assay

In this case, the procedure was done with the product obtained from the last fraction collection, after it was subjected to a 15 cycle PCR and a denaturizing PAGE.

The assay allowed for a comparison between the affinities of the original library and the selected oligonucleotides. This was done by comparing the fluorescence (emanated by the fluorophore contained in one of the primers) of both templates when bound to an affinity column that contains the target[r].

[r] Protocol described in chapter 4, section 4.10.

### 2.3.1. Flow Through, Washing Procedures and Target-bound Sequences

The first result yielded was in regard to the flow-through, meaning the excess of template that did not bind to the target when the incubation took place.

Regarding the flow through, the library had a much bigger fluorescence than the selected oligonucleotides.

When washing the column, both the bulk aptamers and the library showed a significant fluorescent unit value in the first wash, which then decreased dramatically. This is representative of the many molecules that, in both cases, leave the test tube. Regarding the column, only the selected oligonucleotides showed any fluorescence. Table 2 depicts the numerical values obtained in the procedure.

**Table 2 – Overall numerical results obtained in the affinity assay.** The table depicts the fluorescence values (fluorescence units) of the different samples used in the assay- original DNA library, selected aptamers and the sample buffer.

| | Flow Through | First Wash | Second Wash | Third Wash | Affinity Column | Total Fluorescence |
|---|---|---|---|---|---|---|
| **DNA Library** | 586.3 | 39.7 | 4.5 | 1.9 | 0 | 632.4 |
| **Selected Aptamers** | 313.0 | 37.9 | 8.6 | 2.1 | 1.3 | 362.9 |
| **Sample Buffer** | 0.0 | 0.0 | 0.0 | 0.0 | 0.0 | 0.0 |

Regardless of the values obtained for what did not bind at all to the target and/or what left during the washing procedures, one can easily see that there was an improvement, regarding the affinity, during the two selection cycles. Figure 28 depicts a comparison between the fluorescence of the beads when in the presence of the original DNA library and the selected aptamers, indicating that the aptamers did bind to the target.

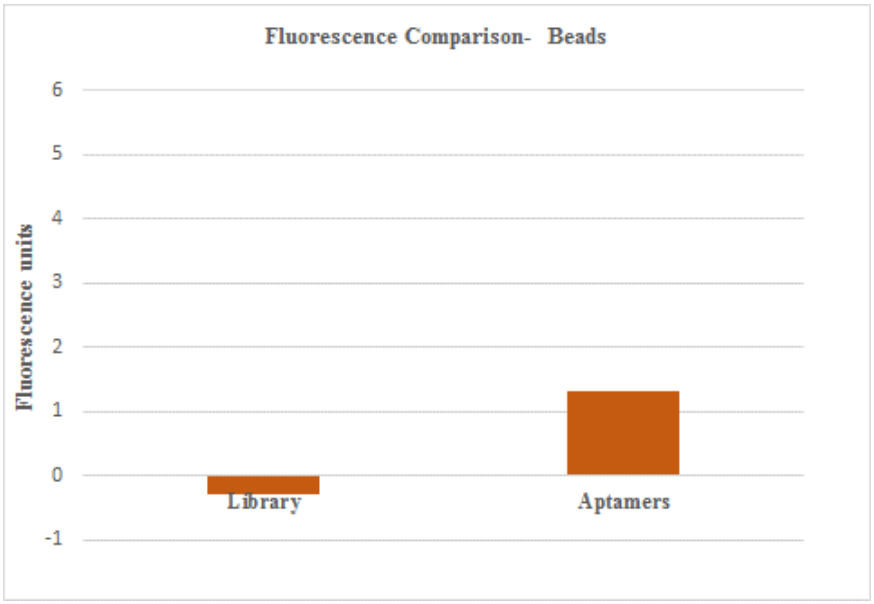


**Figure 28 - Comparison between the affinity results obtained with the original library and the selected aptamers**. The fluorescence (in fluorescent units) of the affinity column increased from 0 to approximately 1.3.

The results obtained can be summed up in Table 3, where the total affinity of the original random library is compared to that of the selected aptamers. The result is obtained by dividing the fluorescence of the column by the total fluorescence of the sample (which is the sum of all its fluorescence values). It is observable that the selected aptamers do have affinity for the target, contrary to the original library.

**Table 3 – Data comparison regarding the affinity measurement assay**. The values obtained for the total affinity were obtained by dividing the fluorescence obtained with the beads by the total fluorescence of the sample (which is the sum of all its fluorescence values).

| Parameters | Original ssDNA | Selected aptamers |
|---|---|---|
| Total Fluorescence (TF) | 632.4 | 362.9 |
| Beads Fluorescence (BF) | 0 | 1.3 |
| Total Affinity (BF/TF) | 0 | $0.4x10^{-2}$ |
| Total Affinity (%) | 0 | 0.4 |

# Chapter 3

## Discussion

### 3.1. General Considerations

Given the vast roles Bk plays in the human body, synthesizing an aptamer that binds to it can be seen as an important advance not only in human biochemistry but, also, in molecular medicine. On the other hand, given how promising these molecules are, as diagnostic, therapeutic and analytical tools, improving how they're synthesized presents itself as both an incredible and exciting challenge [23,14,39,40].

Today, the vast majority of aptamers are synthesized using the conventional SELEX technique, which might be the reason why there aren't that many[46]; making it imperative to improve the aforementioned technique. This way, a new and more efficient tool will be available for diagnostics and treatment within the medical community.

The assays performed in this project were rather conclusive in regard to the viability of using capillary electrophoresis to select aptamers against Bk. However, the real affinity of the selected oligonucleotides must be measured using the synthesized aptamers.

### 3.2. Preliminary Target Analysis

The assay conducted with the FlexStation apparatus yielded the results one might have expected, considering both the peptide and buffer used, and the wavelengths in which the aforementioned assay was performed were adequate. Both the buffer, analyzed in the blank assay (Figure 9 a), and the peptide (Figure 9 b and c) absorb at 214nm, the latter being due to the peptide bonds, as expected.

Whereas the blank assay allows us to understand any influence the buffer might have in this experiment, the results obtained in Figure 9 b and c show, besides the 214nm absorption peak, two others- one near 230nm and another near 260nm- are fairly noticeable; the latter being most likely due to the Phe residue- one of the three amino acid residues, alongside tryptophan and tyrosine, primarily responsible for the inherent absorbance of proteins, whose absorbance can only be observed in the absence of both tryptophan and tyrosine[75].

Regarding the descending, yet considerable, values from 214 to 230, it could be simply due to the peptide's molecular rearrangement; although this is more visible in proteins[76].

The last figure (Figure 9 c), containing only the target in a considerably high concentration, yielded an interesting result, which ties-in with the previous analysis- the maximum lambda shows up at around 260nm and, since no buffer was added, any and all absorbance at 214nm is due to the peptide bonds. When considering all this, one concludes that the peptide is, indeed, pure and adequate for analysis, plus, we can conclude that the wavelength corresponding to the

peptide bonds (214nm) is appropriate for CE analysis, since it revealed no interference and high absorbance.

### 3.3. Capillary Electrophoresis- Method Development and Subsequent Analysis

Developing an appropriate method, using CE, to develop aptamers for bradykinin has proven to be an incredible challenge. The unlimited number of buffer configurations that one may try, presents itself as the biggest challenge, due to the fact that the target and the DNA have very different behaviors when subjected to a CE assay. Most importantly, the conditions in which the folding of the ssDNA occurs may determine not only its behavior during the CE assay but, also, that of the ssDNA-target complex.

#### 3.3.1. Bk

The target's preliminary assay in the FlexStation served as a complementarity assay to that performed with the CE apparatus.

At 214nm, the results obtained with the CE reveal that though the buffer does absorb in this very same wavelength (as discussed above), the peptide itself shows absorption in that very same wavelength, which is in accordance with what had been seen before. In regard to the detection time, as expected due to its small size and considerable charge in these conditions, the peptide moved rather fast, being detected at around 2min, when compared to the ssDNA that presented a detection time of around 10min.

Being a technique that depends on charge-to-size ratio, it is no surprise that a small peptide such as BK, with a PI close to 11, moves so easily. In general, small peptides consisting of just a few amino acids "behave" rather well in such situations and their electrophoretic migration (mobility) can be predicted based on their size and charge characteristics[42]. Another interesting result yielded from this assay was the peak attributed to the interaction between the separation buffer (borate) and the sample buffer- the first being known to interact with salts[77]. An interaction that, apparently, also occurred when another protein (CD73) was submitted to the same assay, under the same conditions.

Still in regard to buffers, when using untreated fused-silica capillaries, the use of high-pH buffers generally produces fast separations because the electroosmotic flow (EOF) is high[42], which explains why the peptide shows up so soon, when compared to the DNA- being smaller and positively charged, it migrates easier, since it ends up being "carried" by the EOF, which flows in the same direction, and the polarity, which was set-up as normal.

The peak attributed to the peptide is not as well defined as would be preferable, which was more noticeable in the second selection round. This was most likely due to the capillary's length[43] (which was reduced in half during the second round) and adsorption- an effect that results from the fact that the analyte and the capillary's silica have opposite charges. Since no actual particle separation occurred during these assays (no mixtures were being analyzed and the composition of the solutions was known), changing the current and/or the elecroosmotic flow (EOF) would not be as effective as increasing the capillary's length (which would then increase the run time)[78]. In fact, both the current and the EOF were in accordance to what should be used given the type of analysis[42].

When considering all this, one can safely assume that the target is viable for this type of analysis. Not only because of its absorption wavelength, which corresponds to that of a peptide, but, also, due to its detection time, which differs considerably from that of the DNA; meaning that a viable collection window can be designed.

In the light of what is known about the technique and the peptide, the results obtained demonstrate that the path chosen was adequate.

### 3.3.2. ssDNA

Nucleic acids are generally electrophoresed in neutral or basic buffers (in low pH buffers, polynucleotides are insoluble in water)[41]. Therefore, the analysis that took place did not yield any type of problems in this matter, as both buffers had pH values over 7 (the run buffer, in particular, had a pH over 9).

Nonetheless, analyzing the DNA posed a much bigger problem than analyzing the target. In fact, even though the method development has to occur whenever a new target presents itself, it is the DNA (whether a newly synthesized library or a pool that has already been subjected to a few rounds of selection) that responds the most to variations in the experimental conditions; especially if the target is a small peptide, such as bradykinin, since its electrophoretic behavior is not that much affected[s]. In most applications of CE involving this type of molecules, untreated, fused-silica capillaries such as the one used are the top choice and the detection window is positioned near the negative electrode which coincides with what was done.

When the capillary is filled with solution, a negative charge on the wall surface prevails- this was obtained with the use of NaOH during the conditioning.

The direction of the EOF in an untreated capillary is always toward the cathode. When a neutral buffer (e.g., phosphate, pH 7) is used for nucleotide separations, the electrophoretic flow forces the negatively charged nucleotides toward the anode, opposite to the direction of the EOF.

[s] As can be seen in the plots presented in appendix A

Detection of the nucleotides will only take place if the existing EOF is larger than the electrophoretic flow[41]. These conditions were obtained through the use of borate (pH 9.3) as the separation buffer, making it safe to assume that, even though the resolution was low, the conditions were appropriate for this kind of analysis- the DNA was easily detected, showing a migration time of around 8min.

The presence of more than one peak in its electropherograms can be due to impurities that persisted after DNA precipitation and extraction, or the primer (which is much less likely due to the fact that a denaturizing PAGE was conducted prior to the CE assay). However, when the concentrations varied, the peak areas revealed to also vary in accordance. The analysis was done by normalizing all areas- all were divided by the smallest value- and plot the normalized values with each respective concentration. In both cycles, the values obtained for the correlation show a very close-to-linear variation (as can be seen in both Figure 13 and Figure 19).

DNA folding is one characteristic that reflects the most how different separating conditions may influence the analysis, especially when compared to a small peptide as Bk.

According to *Biochemistry,* by Donald Voet and Judith G. Voet (3rd edition), Cyrus Levinthal noted that, because of the very large number of degrees of freedom in an unfolded polypeptide chain, the molecule has an astronomical number of possible conformations.

When studied outside the cell, the slowest folding proteins require many minutes or hours to fold primarily due to proline isomerization, and must pass through a number of intermediate states, like checkpoints, before the process is complete.

Even though DNA is not a protein; it makes sense to think that its folding process is just as much affected by all the external factors associated with this technique, especially because it is the DNA that contains the aptamers that will, eventually, bind to the target which, being a small peptide such as Bk, does not behavior so “erratically”. This may also be a good explanation as to why the electropherograms show more than one peak in the ssDNA analysis.

### 3.3.3. DNA-Target Complex

After defining the appropriate conditions, analyzing and collecting the aptamers did not pose a problem.

Interestingly, the peaks yielded during the DNA-target analysis (in both runs) are quite similar to those obtained when analyzing the original library, as seen in ***Figure 29***:

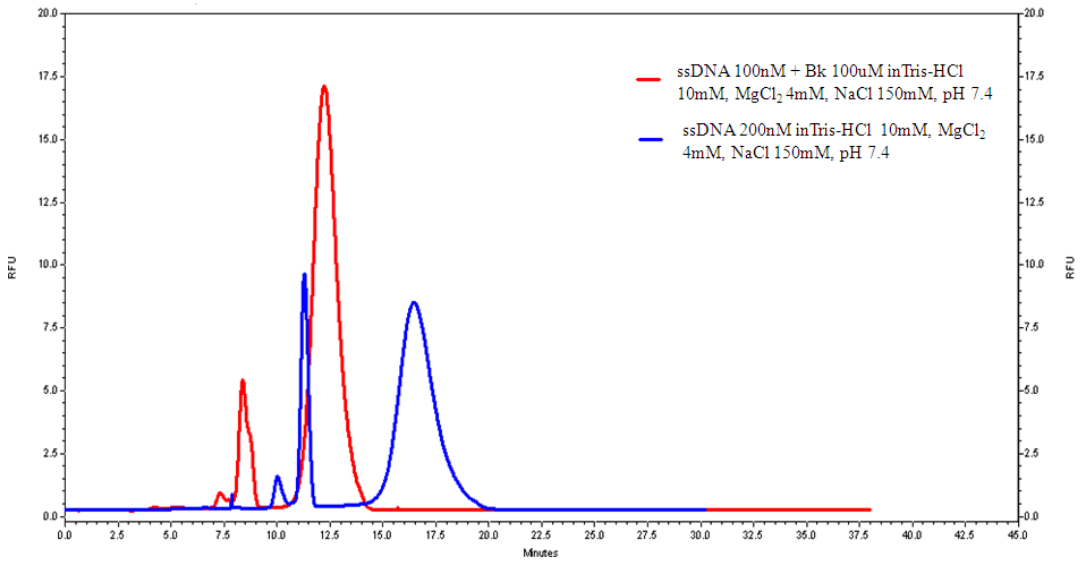


**Figure 29 - Overlay of both the ssDNA and ssDNA-target complex peaks.** The similarities are rather clear. Not just because of the conformations represented but, also, due to the detection time both samples presented. Both analytes are in the same buffer- tris-HCl 10mM, $MgCl_2$ 4mM, NaCl 150mM, pH 7.4. Capillary: 30cm total length, 7um ID, 375um OD. Separation buffer: borate 25mM, pH 9.3.

The lack of a specific complex peak throughout the whole experiment can be attributed to the low number of selection cycles. Since there aren't that may sequences with a significant affinity, the number of DNA-target complex molecules is expected to be low and, therefore, not manifest itself that much (or at all)[54].

It is possible that the peak would present itself after a few more rounds of selection, as shown in Figure 30.

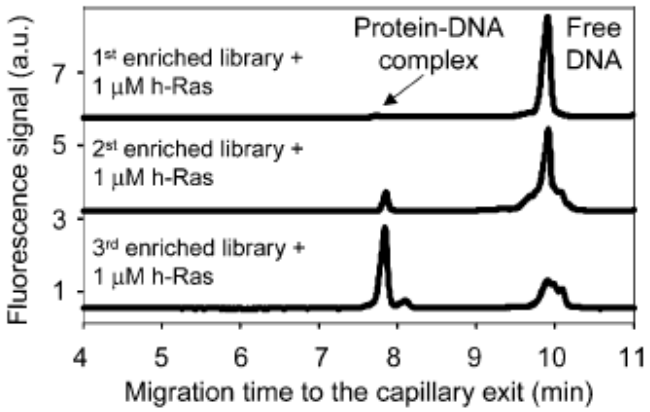


**Figure 30 - NECEEM binding analysis for the determination of bulk $K_d$ of three aptamer-enriched DNA libraries** [54]. The schematics depict the area variations of both the free DNA and the protein-DNA complex as the enrichment cycles proceed.

It could also be that the amount of target used in incubation was not enough to make the DNA-target complex visible.

On the other hand, studies have shown that, even with considerable amounts of target, the complex may not present itself. Therefore, it could be that the lack of a specific peak can be simply because the electrophoretic behavior of the complex is not that different from that of the free DNA [54].

In this case, variations in the far-righted peak (independent of concentration) was also seen (Figure 14). However, significant differences can be seen in the absorption units yielded by the laser induced fluorescence, which can be attributed to the changes induced by the presence of the target. That, as well as the difference in migration times, might indicate the presence of the DNA-target complex. This was further corroborated by the negative selection (see below). One possible explanation for this is that the fluorescence of fluorophore used (FitC) might have been hindered at some point during analysis. Either due to the molecule's conformation or due to some sort of reaction with the buffer.

In order to define a good collection window, when no complex peak can be seen, one has to analyze the migration times of both the target and the DNA. Typically, these parameters can be found from a single assay[51,56].

Considering this, it would seem that the collection window used in both cases was adequate, since both positive and negative selection (Figure 7) proved that no unbound DNA was collected, meaning that any genetic material obtained was, in fact, the product of a successful selection.

### 3.3.4. $K_d$

Even though the bulk $K_d$ cannot be measured when one has a highly heterogeneous DNA library, it does allow to measure the abundance of aptamers within the aforementioned DNA pool; which means it is, indeed, a good way to qualitatively monitor the progress of the selection process[47]. In fact, the values obtained for the bulk $K_d$ reveal that the selection process is progressing well, given that it decreased from 73μM to 54μM[t] in the second selection cycle- a reduction of nearly 26%.

Also, one must bear in mind that the latter value was obtained not with the synthesized aptamers, but with the bulk product obtained directly from the collection process- this means that it is representative of all the sequences present in the mixture and not of the 16 obtained with the sequencing procedure.

The analysis should be repeated, using the synthesized aptamer, thus yielding a more accurate $K_d$ instead of a bulk one.

## 3.4. DNA Sequencing

The sequencing procedure yielded very interesting results. Ones that reveal that, indeed, there was a considerable selection of genetic material during this process.

Of the 100 colonies used, 16 sequences with considerable similarities were obtained, when using ClustalW2. The fact these sequences present so many similarities, in itself, indicates the success of the selection process. Furthermore, this is confirmed by the aptamers' secondary structure[u]. The repeated motifs amongst the elements of each group (and between groups) indicate that the selection was a success.

## 3.5. Affinity Assay

This assay intended to demonstrate whether or not the two selection cycles allowed for a significant improvement in the number of sequences that have affinity for the target, thus binding to it.

Regardless of the values obtained for what did not bind at all to the target and/or what left during the washing procedures, one can easily see that there was an improvement, regarding the affinity, during the two selection cycles. Figure 28 allows a comparison between the fluorescence of the beads when in the presence of the original DNA library and the selected

[t] Refer to chapter 4, section 4.8, for further reference on how this value was obtained.
[u] Presented in chapter 2, section 2.2.

aptamers. The difference is clear- the aptamers did bind to the Bk, which allows us to conclude that the selection was a success, in spite of the measuring having been done with the bulk aptamers.

### 3.6. Final Remarks

The main focus of this project was to develop a method for aptamer selection, against Bk, using CE, given that the use of CE has proven to be effective and to make the whole process faster. Capillary electrophoresis allowed, with just two selection rounds, to obtain a pool of DNA that does bind to its target. Not only that, the decrease in the $K_d$ value reveals that the selection process with the CE technique did perform well.

The sequences obtained contain repetitive bases; plus, the structures reveal repeated motifs, which indicates that there was, indeed, a significant level of selection. This statement can also be corroborated by the increase of affinity seen in the fluorescence assay- the original library had no fluorescence at all when the analyzing the beads and the bulk aptamers presented an overall binding ratio of 0.4%[v].

Analyzing the synthesized aptamers is definitely crucial in order to infer any definite conclusions regarding the process that lead to the development of these molecules. However, the results obtained are promising indicators of the viability of the whole selection process behind the development of these molecules. Therefore, the obtained oligonucleotides represent viable options for creating a diagnostic kit intended to measure Bk plasma concentrations and/or its metabolites given the significant affinity that the bulk product revealed, hence contributing to new prospects on identification and/or treatment of various diseases related to pathophysiologic and pharmacologic alterations in systemic bradykinin generation.

Also, these results open doors regarding the development of complementary diagnostic kits for Bk's metabolites, such as Bk 1-5 and Des-Arg9-Bk, also involved in known human conditions.

[v] This value is obtained by dividing the fluorescence in the beads by the overall fluorescence of the sample, as seen in section 2.3.1.

# Chapter 4

## Materials and Methods

### 4.1. Bradykinin Absorbance Spectre

This assay required, simply, the already mentioned equipment and a 96 well plate. Three wells were used, all filled with 200ul solutions:

- A1 was filled with the following solution (posing as the blank assay), which was expected to absorb at 214nm: 20ul 10x buffer+6.6 µl 1.5M NaCl+173.4µl H2O.
- A2 was filled with the following solution, which was expected to absorb at 260nm due to the fact that this peptide has 2 phenylalanine residues: 4µl 50mM Bk+20µl 10x buffer+6.6µl 1.5M NaCl+169.4µl H2O.
  This solution had a Bk concentration of 1mM.
- A3 was filled with an over-concentrated 200µl of 50mM Bk in water (no buffer was used), in order to confirm the results regarding the absorption wavelength of this peptide.

### 4.2. Standard PCR for library amplification

The described protocol is the lab's standard procedure:
For a total volume of 3000µL, 50µl of milliQ grade water were mixed with 20µl of 5M betaine, 5µL of DMSO 100%, 10µL of 10x taq buffer $(NH)_4SO_4$, 10µL of 25mM $MgCl_2$, 2µL of Life Technologies' 10mM dNTP mix (premixed aqueous solutions of dATP, dCTP, dGTP and dTTP), 1µL of each primer 100pmol/µL[w], 1µL of enzyme taq polymerase (Life Technologies) and 2µL of the appropriate DNA template (1fmol/µL).
All this was centrifuged, so it would settle appropriately and, then, submitted to the thermocycler program desfribed in Table 4.

[w] Modified forward and reverse primers- one containing a fluorescente marker (FitC) and another containing a PolyA tail, respectively. These modifications allow, respectively, a better visualization of the DNA in the CE and PAGE and a better strand separation when submitted to a denaturizing gel.
FitC Primer sequence: GGGAGACAAGAATAAGCG
PolyA primer sequence: GCCTGTTGTGAGCCTCCT

**Table 4 - Thermocycler program for library amplification**. Steps 2, 3 and 4 were repeated 14 times.

| *Temperature (ºC)* | *Time* |
|---|---|
| 95 | 4min |
| 95 | 45sec |
| 42 | 45sec |
| 72 | 2min |
| 72 | 10min |

### 4.3. Polyacrylamid Gel Electrophoresis (PAGE)

In order to confirm the viability of any amplified genetic material, the product obtained from the PCR was submitted to a PAGE analysis. The gel itself was obtained by mixing 10.5mL of milliQ water with 1.5mL of 10x TBE buffer, 3mL of 40% acrylamide, 150µL of 10% APS and 15µl of TEMED (Life Technologies). This mixture was, then, poured on the Novex Gel Cassette (Life Technologies). After this, the comb was added (the number of wells depends on the number of samples).

Once ready, the samples were mixed with the appropriate dye (6x blue dye, by Life Technologies) and introduced inside the wells. The ladder (100 base pairs ladder, by Life Technologies) was introduced in its own well. It ran for about 2 hours at 100V, using 1x TBE as the run buffer. When finished, the gel was unmounted and submerged in a mixture of 5µL of SYBR Safe DNA gel stain (Life Technologies) and 50 mL of run buffer. It was gently stirred for 20min, at room temperature, whilst submerged in this mixture.

### 4.4. DNA denaturation/strand separation

Once the DNA was considered viable, it was submitted to a denaturizing gel in order to yield the desired single-stranded DNA.

The genetic material was precipitated using 10% glycogen (0.1% m/v), 10% 3M Sodium Acetate pH 7.4 and 5% 1M $MgCl_2$. After vortexing, cool ethanol 100% was added so that its concentration becomes 75% of the total volume obtained. The mixture was incubated at -20°C overnight. After this, it was centrifuged for 30 min at 4°C at full speed (13200rpm) and the over floating product was discarded. 750 µL of cool ethanol 70% were added and the mixture was centrifuged for 5min at full speed and 4ºC. This step was then repeated.

After discarding the over floating product, the pellet was left to dry at room temperature. Once dry, sterile water was added in small amounts until the total volume, in μL, added up to 10 times the number of reactions made.

For the strand separation, a denaturizing gel (8%) was prepared by mixing 10mL 10x TBE buffer, 20 mL of 40% acrylamide, 70 mL of 12M urea, 500μL 10% APS and 50 μL TEMED (Life Technologies).

Once ready, a pre-run was made- the gel is turned on, for 30min, at 400V. This step is done to ensure that the template does not cool down once it enters the wells. While this was happening, the sample was heated at 95ºC, after being mixed with formamide 1:1 and loading dye buffer 6x (Life Technologies). Once ready, the sample was introduced, with the ladder (100 base pairs ladde, by Life Technologies), inside the wells (only one well was used, in order to increase DNA/gel ratio when cutting it off), and let run at 300V for about 3 hours, using TBE buffer 1x as the run buffer.

When finished, the gel was dyed with 5μL SYBR Green RNA (Life Technologies) stain in 50 mL of run buffer for 20min. It was then analyzed under a UV light and the adequate band (the one corresponding to the strand marked with FitC) was cut off.

### 4.5. DNA Extraction/Purification with Phenol and Chloroform

The gel was smashed until a homogenous gel-O-like mixture was obtained. Then, 1 mL of water milliQ and 1mL of phenol were added. After vortexing for 30min it was centrifuged for 10min at full speed, at 4ºC. The aqueous phase (over floating phase) was transferred to another tube (while the remaining product was discarded) and had chloroform added to it (1:1).

The mixture was vortexed for 10sec and centrifuged for 5min at full speed (13200rpm) and 4ºC. After this, the precipitation protocol used was the one described in 4.4.

### 4.6. ssDNA Folding and ssDNA-Target Complex Formation

Having the ssDNA ready, the appropriate amount was mixed with the desired buffer. The mixture was incubated in the thermocycler at 95° for 20min and then at 25°C for 20min.

The complex is obtained by incubating the ssDNA with the target for 15min once the aforementioned procedure is completed. The amount of ssDNA and/or target used in the incubation depends on the desired concentration. In this case, both cycles were done using the same proportions of ssDNA and Bk- 100nm ssDNA+ 100μM Bk. It is important that the target has a much higher concentration- this ensures that a great number of sequences bind to it.

### 4.7. Capillary Electrophoresis (Bk, DNA and DNA-target complex)

All runs, regardless of the substrate (target, DNA and DNA-target complex), were performed using the Beckman Coulter PA 800. The voltage used was 0.3V/cm. The maximum current was 300uA. The separation buffer used was sodium borate ($Na_2B_4O_7$) 25mM, pH 9.3 (common use).
All target-related assays were conducted using 214nm wavelengths, with the UV detector.
All DNA and/or DNA-target complex assays were conducted with a LIF (Laser Induced Fluorescence) detector, with an excitation wavelength of 488nm and an emission wavelength of 520nm.
All runs in the first selection cycle were conducted using a fused silica capillary, 60cm in total length, 50cm from injection point to detection point.
All runs in the second selection cycle were conducted using a fused silica capillary, 30cm in total length, 20cm from injection point to detection point.
Both capillaries had both an internal and outer diameter of 75 and 375µm, respectively.
The designed method starts off with intensive capillary conditioning. This is crucial, especially if the capillary is new.
Although usually underestimated, the conditioning allows for good reproducibility. When using a non-coated fused silica capillary, it is important to understand the nature of the charge in the walls. At pH above 3, the electroosmotic flow becomes an important factor, due to the fact that the capillary becomes charged[79]. The conditioning procedure should also be used if, for some reason, the capillary is put out of use for a few days, in order to ensure the aforementioned reproducibility.
In this case, it was done as presented in Table 5.

**Table 5 - Conditioning Procedure for Capillary Electrophoresis.**

| ***Reagent*** | ***Time (min)*** |
|---|---|
| Water (miliQ grade or better) | 10 |
| NaOH, 25nM | 10 |
| Water (miliQ grade or better) | 2 |
| NaOH, 25nM | 10 |
| Water (miliQ grade or better) | 2 |
| Sample buffer | 10 |

After the conditioning, the run method was performed, as described below. It is the same for all analytes- target, DNA and DNA-target complex.

**Table 6 – Program designed within the CE apparatus.** Depiction of all events programed within the equipment's software that lead to the analysis of all three samples- target, DNA and DNA-target complex. BI and BO represent the "in" and "out" trays. SI is the special inlet tray, which is usually used to store the sample, since it enters a special chamber with regulated temperature. A1 through E6 are the codes that represent the various positions within each tray, all containing a specific vial with the referred product. The separation buffer used was borate pH=9.3. The sample buffer used is Tris-HCl 10mM, $MgCl_2$ 4mM, NaCl 150mM, pH 7.4

| *Event* | *Value* | *Duration* | *Inlet Vial* | *Outlet Vial* |
|---|---|---|---|---|
| Rinse-Pressure | 20.0 Psi | 5.00 min | BI:A1 (Water MiliQ) | BO:A1 (Waste) |
| Rinse-Pressure | 20.0 Psi | 5.00 min | BI:A3 (SDS 1%) | BO:A1 (Waste) |
| Rinse-Pressure | 20.0 Psi | 5.00 min | BI:A1 (water MiliQ) | BO:A1 (Waste) |
| Rinse-Pressure | 20.0 Psi | 20.0 min | BI:A2 (NaOH 10mM) | BO:A1 (Waste) |
| Rinse-Pressure | 20.0 Psi | 2.00 min | BI:A1 (Water MiliQ) | BO:A1 (Waste) |
| Rinse-Pressure | 20.0 Psi | 10.0 min | BI:C1 (Separation Buffer) | BO:A1 (Waste) |
| Inject-Pressure | 3.0 Psi | 13.0 sec | SI:E6 (Sample) | BO:A3 (Water MiliQ) |
| Separate-Voltage | 18kV/9kV | 30.0 min | BI:C1 (Separation Buffer) | BO:C1 (Separation Buffer) |
| End | | | | |

### 4.8. Determining the $K_d$ and the Collection Window

Both the $K_d$ and the aptamer collection window were obtained as detailed in consulted literature[47]. However, a few alterations (regarding $A_1$, $A_2$ and $A_3$) had to be made so that the $K_d$ could be determined more accurately.

Given that no specific peak was obtained when analyzing the aptamers, the $A_2$ parameter was given a null value. Regarding the $A_1$ and $A_3$ parameters, for the ssDNA and the ssDNA-target complex respectively, both were obtained through the following steps:

- For each specific electropherogram (there's one for each concentration used regarding the same analyte), an average value was calculated for the overall area, adding the values of each peak and dividing the obtained value by the number of peaks in each electropherogram. This was done for each concentration presented and for both analytes (ssDNA and Bk).
- Using the values that resulted from the previous step, a new average value was calculated- they were all summed and the obtained value was divided by the number of electropherograms in the graphic. This value is to be considered the "actual area" of the peak of that specific analyte (again, this was done for both analytes). It's as if that analyte yielded only one peak and this value represents its area.
- The values obtained in the previous step were, then, considered either $A_1$ or $A_3$, depending on what analyte was being taken into consideration- ssDNA or the ssDNA-target complex, respectively (again, $A_2$=0).

### 4.9. Aptamer sequencing

*Escherichia coli* XL1 Plus competent cells used to obtain plasmid constructs were obtained following the calcium chloride ($CaCl_2$) method [80].

The plasmid was incubated with 4µL of aptamers with a concentration of around 200ng/µL, 1µL of plasmid and 1µL of saline solution (all from TOPO Cloning Kit 2.1).

Transformations were performed by incubating *E. coli* with approximately 80ng of DNA on ice for 30min, followed by a heat shock at 42ºC (2min) and incubation on ice for 2min. 500µl of Life Technologies' liquid LB medium (lysogeny broth medium) were added, followed then by incubation at 37ºC, with gentle shaking (230rpm). Transformed cells were plated in LB-agar medium (lysogeny broth and agar medium) with 50µg $ml^{-1}$ ampicillin and incubated overnight at 37 ºC.

After this, the viable colonies were placed in PBS 1x and submitted to the lab's standardized colony PCR protocol: in each well, 10mM dNTP, 15mM primer M13 forward, 24.9mM primer M13 reverse, 25nM $MgCl_2$, 1x Taq polymerase buffer, 5U/uL taq polymerase and water were added. After this, the plaque was submitted to the thermocycler program depicted in Table 7.

**Table 7 – Thermocycler program used for colony PCR**

| ***Temperature (ºC)*** | ***Time*** |
|---|---|
| *95* | 4min |
| *95* | 45sec |
| *42* | 45sec |
| *72* | 2min |
| *72* | 10min |

After this, the product obtained in each well was submitted to the lab's standard pre-sequencing PCR: 350ng of aptamers were mixed with 3uL of 3.2pmol/µL primer M13 forward, 3µL of 5x sequencing buffer, 2µL of big Dye (all from the Biosystem's Terminator Big Dye 3.1 kit). In the end, water was added until a total volume of 15uL was obtained. The thermocycler program used is represented in Table 8.

**Table 8 – Thermocycler program used for sequencing PCR.**

| *Temperature (ºC)* | *TIME (min)* |
|---|---|
| *96* | 2min |
| *96* | 45sec |
| *50* | 30sec |
| *60* | 4min |
| *4* | Hold |

Following the PCR, the product obtained was precipitated, dried and re-suspended in water in order to be sent to the sequencing lab.

### 4.10. Affinity Assay

In order to retain maximum binding capacity of the pre-activated sepharose medium, all solutions used were in a temperature between 0ºC and 4ºC. Also, the time-interval between steps was minimized as much as possible.

First, the ligand (Bk 100 µM in in tris-HCl 10mM, $MgCl_2$ 4mM, NaCl 150mM, pH 7.4) was dissolved in the appropriate buffer (0.2M $NaHCO_3$, 0.5M NaCl pH 8.3).

As soon as the NHS-activated Sepharose 4 Fast Flow (Sigma Aldrich) was washed with 10 to 15 medium volumes of cold 1mM HCl, it was put to use immediately.

The washed medium was, then, mixed with the coupling solution (ssDNA 100 nM in in tris-HCl 10mM, $MgCl_2$ 4mM, NaCl 150mM, pH 7.4) and the pH was adjusted (maintained between 6 and 9).

The coupling took place on the bench, at room temperature, during 3 hours (the recommended time is between 2 to 4h).

Once the coupling was completed, all non-coupled groups in the medium were blocked through the use of 0.5M ethanolamine, 0.5M NaCl pH 8.3. Then, the medium was washed with two alternate solutions with high and low pH- 3x1 medium volumes 0.1M Tris-HCl pH 8 to 9 and 3x1 volumes 0.1M acetate, 0.5M NaCl pH 4 to 5. After this, the affinity was measured in the FlexStation 3 apparatus.

In order to determine the increase of affinity due to the performed selection cycles, the fluorescence values obtained with the beads were divided by the overall fluorescence value obtained for the specific sample.

**References:**

(1) Ulrich, H. e Trujillo, C. . (2008) Aptâmeros: uma nova ferramenta biotecnológica, in *Bases Moleculares da Biotecnologia, 1st edition* 1st ed., pp 37–54.

(2) Tuerk, C., and Gold, L. (1990) Systematic evolution of ligands by exponential enrichment: RNA ligands to bacteriophage T4 DNA polymerase. *Science 249*, 505–510.

(3) Ulrich, H., Ippolito, J. E., Pagán, O. R., Eterović, V. a, Hann, R. M., Shi, H., Lis, J. T., Eldefrawi, M. E., and Hess, G. P. (1998) In vitro selection of RNA molecules that displace cocaine from the membrane-bound nicotinic acetylcholine receptor. *Proc. Natl. Acad. Sci. U. S. A. 95*, 14051–14056.

(4) Ellington, A.D. e Szostak, J. (1990) In vitro selection of RNA molecules that bind specific ligands. *Nature 346*, 818–22.

(5) Dieckmann T, Suzuki E, Nakamura GK, F. J. (1996) Solution structure of an ATP-binding RNA aptamer reveals a novel fold. *RNA* 628–640.

(6) Huizenga DE, S. J. (34AD) A DNA aptamer that binds adenosine and ATP. *Biochemistry 2*, 656–665.

(7) Burke DH, G. L. (1997) RNA aptamers to the adenosine moiety of S-adenosyl methionine: structural inferences from variations on a theme and the reproducibility of SELEX. *Nucleic Acids Res 25*, 2020–4.

(8) Mercey R, Lantier I, Maurel MC, Grosclaude J, Lantier F, M. D. (2006) Fast, reversible interaction of prion protein with RNA aptamers containing specific sequence patterns. *Arch Virol 151*, 2197–214.

(9) Ulrich H, Trujillo CA, Nery AA, et al. (2006) DNA and RNA aptamers: from tools for basic research towards therapeutic applications. *Com Chem High Throughput Screen 9*, 19–32.

(10) Ulrich H, Martins AH, P. J. (2004) RNA and DNA aptamers in cytomics analysis. *Cytom. A 59*, 220–31.

(11) Ulrich, H. e. al. (2005) RNA and DNA aptamers in cytomics analysis, in *Current Protols in Cytometry*, pp 28.1–7,28.39. John Wiley & Sons, Inc.

(12) Gold, L. et al. (2012) Aptamers and the RNA world, past and present. *Perspect. Biol 1.4*.

(13) Shamah, S. M. et al. (2008) Complex target SELEX. *Acc. Chem. Res 41*, 2142.

(14) GJ, W. (2007) Monoclonal antibody mechanisms of action in cancer. *Imunol Res 39*, 271–8.

(15) Ulrich H, W. C. (2009) Disease-specific biomarker discovery by aptamers. *Cytom. A*.

(16) Wilson, D.S. & Szostak, J. . (1999) In vitro selection of functional nucleic acids. *Annu. Rev. Biochem. 68*, 611–647.

(17) Famulok, M., Mayer, G. & Blind, M. (2000) Nucleic acid aptamers—from selection in vitro to applications in vivo. *Acc. Chem. Res 33*, 591–599.

(18) Rimmele, M. (2003) Nucleic acid aptamers as tools and drugs: recent developments. *Chembiochem 4*, 963–971.

(19) Lee, J. F., Stovall, G. M., and Ellington, A. D. (2006) Aptamer therapeutics advance. *Curr. Opin. Chem. Biol. 10*, 282–289.

(20) RT, B. (2006) Structures of regulatory elements in mRNAs. *Curr Opin Struct Biol 16*, 299–306.

(21) RR, T. B. B. (2005) Riboswitches as versatile gene control elements. *Curr Opin struct Biol 15*, 342–48.

(22) Nudler E, M. A. (2004) The riboswitch control of bacterial metabolism. *trend Biochem 29*, 11–7.

(23) Ulrich H, W. C. (2013) Identification of aptamers as specific binders and modulators of cell-surface receptor activity, in *Methods Bol. Biol.*, pp 187–214.

(24) Germer, K., Leonard, M., and Zhang, X. (2013) RNA aptamers and their therapeutic and diagnostic applications. *Int. J. Biochem. Mol. Biol. 4*, 27–40.

(25) Tombelli, S., Minunni, M., and Mascini, M. (2005) Analytical applications of aptamers. *Biosens. Bioelectron. 20*, 2424–2434.

(26) Baldrich, E., Restrepo, A., and O'Sullivan, C. K. (2005) Aptasensor development: Elucidation of critical parameters for optimal aptamer performance. *Anal. Chem. 76*, 7053–7063.

(27) Vicens, M. C., Sen, A., Vanderlaan, A., Drake, T. J., and Tan, W. (2005) Investigation of molecular beacon aptamer-based bioassay for platelet-derived growth factor detection. *ChemBioChem 6*, 900–907.

(28) Lai, R. Y., Plaxco, K. W., and Heeger, A. J. (2007) Aptamer-Based Electrochemical Detection of Picomolar Platelet-Derived Growth Factor Directly in Blood Serum variant of PDGF at 1 nM directly in undiluted , unmodified. *Anal. Chem. 79*, 229–233.

(29) Ge, J., Liu, Z., Zhi, Z., and Zhao, X. S. (2011) Qualitative and quantitative thrombin analysis in serum using aptamers and gold nanoparticles through progressive dilution. *Anal. Biochem. 413*, 75–77.

(30) Xiao, Y., Lubin, A. a., Heeger, A. J., and Plaxco, K. W. (2005) Label-free electronic detection of thrombin in blood serum by using an aptamer-based sensor. *Angew. Chemie - Int. Ed. 44*, 5456–5459.

(31) Mir, M., Vreeke, M., and Katakis, I. (2006) Different strategies to develop an electrochemical thrombin aptasensor. *Electrochem. commun. 8*, 505–511.

(32) Bock, C. et al. (2004) Photoaptamer arrays applied to multiplexed proteomic analysis. *Proteomics 4*, 609–618.

(33) Surugiu-Warnmark, I., Warnmark, A., Toresson, G., Gustafsson, J.A. & Bulow, L. (2005) Selection of DNA aptamers against rat liver X receptors. *Biochem. Biophys. Res. Commun. 332*, 512–517.

(34) Pestourie, C., Tavitian, B. & Duconge, F. (2005) Aptamers against extracellular targets for in vivo applications. *Biochimie 87*, 921–930.

(35) Davidson, E.A. & Ellington, A. D. (2005) Engineering regulatory RNAs. *Trends Biotechnol 23*, 109–112.

(36) Nutiu, R., Yu, J.M. & Li, Y. (2004) Signaling aptamers for monitoring enzymatic activity and for inhibitor screening. *Chembiochem 5*, 1139–1144.

(37) Famulok, M. & Mayer, G. (2005) Intramers and aptamers: applications in protein–function analyses and potential for drug screening. *Chembiochem 6*, 19–26.

(38) Patil, S.D., Rhodes, D.G. & Burgess, D. . (2005) DNA-based therapeutics and DNA delivery systems: a comprehensive review. *AAPS J 7*, 61–77.

(39) Nimjee, S.M., Rusconi, C.P. & Sullenger, B. A. (2005) Aptamers: an emerging class of therapeutics. *Annu. Rev. Med 56*, 555–583.

(40) Burnett, J.C. e Rossi, J. J. (2012) RNA-based therapeutics: current progress and future prospects. *Chem. Biol. 19*, 60–71.

(41) McCord, B., Hartzell-Baguley, B., and King, S. (2008) Separation of DNA by capillary electrophoresis. *Methods Mol. Biol.*

(42) Schwartz, H., and Pritchett, T. (1994) Separation of proteins and peptides by Capillary Electrophoresis: Application to Analytical Biotechnology. *Development* (Coulter, B., Ed.) 1st ed.

(43) Skoog, D.A.; Holler, F.J.; Crouch, S. . (2007) Principles of Instrumental Analysis (Publishing, T. B., Ed.) 6th ed. Thomson Brooks/Cole Publishing.

(44) Skoog, D.A.; Holler, F.J.; Nieman, T. A. (1998) Principles of Instrumental Analysis 5th ed. Saunders college Publishing.

(45) Weinberger, R. Practical Capillary Electrophoresis 2nd ed.

(46) Lee, J.F., Hesselberth, J.R., Meyers, L.A. & Ellington, A. . (2004) Aptamer database. *Nucleic Acids Res 32*, 95–100.

(47) Berezovski, M., Berezovski, M., Musheev, M., Musheev, M., Drabovich, A., Drabovich, A., Jitkova, J., Jitkova, J., Krylov, S., and Krylov, S. (2006) Non-SELEX: selection of aptamers without intermediate amplification of candidate oligonucleotides. *Nat Protoc*.

(48) Drolet, D.W., Jenison, R.D., Smith, D.E., Pratt, D. & Hicke, B. (1999) A high throughput platform for systematic evolution of ligands by exponential enrichment (SELEX). *Comb. Chem. High Throughput Screen 2*, 271–278.

(49) Ciesiolka, J., Illangasekare, M., Majerfeld, I., Nickles, T., Welch, M., Yarus, M., and Zinnen, S. (1996) Affinity selection-amplification from randomized ribooligonucleotide pools. *Methods Enzymol. 267*, 315–335.

(50) Petrov, A., Okhonin, V., Berezovski, M. & Krylov, S. N. (2005) Kinetic capillary electrophoresis (KCE): a conceptual platform for kinetic homogeneous affinity methods. *J. Am. Chem. Soc 127*, 17104–17110.

(51) Berezovski, M. et al. (2005) Nonequilibrium capillary electrophoresis of equilibrium mixtures: a universal tool for development of aptamers. *J. Am. Chem. Soc. 127*, 3165–3171.

(52) Berezovski, M. & Krylov, S. N. (2002) Nonequilibrium capillary electrophoresis of equilibrium mixtures — a single experiment reveals equilibrium and kinetic parameters of protein–DNA interactions. *J. Am. Chem. Soc. 124*, 13764–13765.

(53) Berezovski, M. & Krylov, S. N. (2005) Thermochemistry of protein–DNA interaction studied with temperature-controlled nonequilibrium capillary electrophoresis of equilibrium mixtures. *Anal. Chem. 77*, 1526–1529.

(54) Berezovski, M., Musheev, M., Drabovich, A., and Krylov, S. N. (2006) Non-SELEX selection of aptamers. *J. Am. Chem. Soc.*

(55) Mosing, R.K., Mendonsa, S.D. & Bowser, M. . (2005) Capillary electrophoresis-SELEX selection of aptamers with affinity for HIV-1 reverse transcriptase. *Anal. Chem 77*, 6107–6112.

(56) Drabovich, A.P., Berezovski, M., Okhonin, V. & Krylov, S. . (2006) Selection of smart aptamers by methods of kinetic capillary electrophoresis. *Anal. Chem. 78*, 3171–3178.

(57) Mendonsa, S.D. & Bowser, M. T. (2004) In vitro evolution of functional DNA using capillary electrophoresis. *J. Am. Chem. Soc. 126*, 20–21.

(58) Rocha e Silva M, Beraldo WT, R. G. (1949) Bradykinin, a hypotensive and smooth muscle stimulating factor released from plasma globulin by snake venoms and by trypsin. *Am J Physiol. 156*, 261–73.

(59) Cleber A. Trujillo, Priscilla D. Negraes, Telma T. Schwindt, Claudiana Lameu, Cassiano Carromeu, Alysson R. Muotri, João B. Pesquero, Débora M. Cerqueira, Micheli M. Pillat, Héllio D. N. de Souza, Lauro T. Turaça, J. G. A. and H. U. Kinin-B2 Receptor Activity Determines the Differentiation Fate of Neural Stem Cellsle. *PubMed - Index. Medlin.*

(60) C.M. Boulanger, P. M. V. (1998) The endothelium: a modulator of cardiovascular health and disease. *Dialogues Cardiovasc. Med. 3*, 185–244.

(61) Margolius, H. S. (1995) Kallikreins and Kinins Some Unanswered Questions About System Characteristics and Roles in Human Disease. *Am. Hear. Assoc. - Hypertens. 26*, 221–229.

(62) Rhaleb NE, Yang XP, C. O. (2011) The kallikrein-kinin system as a regulator of cardiovascular and renal function. *Compr Physiol 1*, 971–83.

(63) GmbH, H. H. A. P. D. Non-peptide Antagonists and Agonists of the Bradykinin B2 Receptor. *Med. Chem. (Los. Angeles). 65926*.

(64) François Alhenc-Gelas, Nadine Bouby, Christine Richer, Louis Potier, R. R. and M. M. Kinins as Therapeutic Agents in Cardiovascular and Renal Diseases. *PubMed - Idexed Medlin.*

(65) Murphey LJ, Hachey DL, Vaughan DE, Brown NJ, M. J. (2001) Disease Quantification of BK1-5, the stable bradykinin plasma metabolite in humans, by a highly accurate liquid-chromatographic tandem mass spectrometric assay. *Anal Biochem 292*, 87–93.

(66) Murphey, L. J., Malave, H. a, Petro, J., Biaggioni, I., Byrne, D. W., Vaughan, D. E., Luther, J. M., Pretorius, M., and Brown, N. J. (2006) Bradykinin and its metabolite bradykinin 1-5 inhibit thrombin-induced platelet aggregation in humans. *J. Pharmacol. Exp. Ther. 318*, 1287–1292.

(67) Juerg Nussberg, Massimo Cugno, Catherine Amstutza, Marco Cicardi, Andrea Pellacani, A. A. (1998) The Lancet. *Lancet 351*, 1693–1697.

(68) Zou, K., Maeda, T., Watanabe, A., Liu, J., Liu, S., Oba, R., Satoh, Y. I., Komano, H., and Michikawa, M. (2009) Aβ42-to-Aβ40- and angiotensin-converting activities in different domains of angiotensin-converting enzyme. *J. Biol. Chem. 284*, 31914–31920.

(69) Selkoe, D. (2001) Alzheimer's disease results from the cerebral accumulation and cytotoxicity of amyloid\ beta-protein. *J. Alzheimer's Dis.* 75–81.

(70) Hock, F. J., Albus, U., Linz, W., Alpermann, H. G., Anagnostopoulos, H., Henke, S., Breipohl, G., and Knolle, J. (1991) Hoe 140 an new potent and long acting bradykinin-antagonist: in vivo studies 774–777.

(71) Raja SN, Campbell JN, Meyer RA, C. R. (1992) Role of kinins in pain and hyperalgesia: psychophysical studies in a patient with kininogen deficiency. *Clin Sci 83*, 337–41.

(72) Dray, A. (1995) Inflamatory Meadiators of Pain. *Br. J. Anaesth. 75*, 125–131.

(73) Calixto JB, Cabrini DA, Ferreira J, C. M. (2000) Kinins in pain and inflammation. *87*, 1–5.

(74) Sharma, J. N., and AL-Sherif, G. J. (2011) The Kinin System: Present and Future Pharmacological Targets. *Am. J. Biomed. Sci. 3*, 156–169.

(75) Held, P. (2003) Peptide and Amino Acid Quantification Using UV Fluorescence in Synergy HT Multi-Mode Microplate Reader. *BioTek Instruments, Inc*.

(76) Lee, V. Peptide and Protein Drug Delivery.

(77) Krivánková, L., Brezková2, M., Gebauer, P., and Bocek, P. (2004) Importance of the counterion in optimization of a borate electrolyte system for analyses of anions in samples with complex matrices performed by capillary zone electrophoresis. *Electrophoresis 25*, 3406–3415.

(78) Weinberge, R. Chapters 2.5, 2.8, 2.9, 2.10, in *Practical Capillary Electrophoresis*.

(79) Chapman, H. W. and J. Precision in capillary electrophoresis, in *Capillary Electrophoresis: Technical information. T-1860*$^{a}$. Beckman Coulter, Inc.

(80) Dagert, M., and Ehrlich, S. D. (1979) Prolonged incubation in calcium chloride improves the competence of Escherichia coli cells. *Gene 6*, 23–28.

## Appendix A

### A1. Capillary Electrophoresis- Method Development

The following is a gathering of some results obtained whilst still developing the appropriate methodology to use the CE equipment for the selection cycles.

Not all results from all assays will be presented. It is important to note that, during these tests, the folding process was different. Unless stated otherwise, the mixture was incubated in the thermocycler at 85° for 20 min and then at 25°C for 20 min. Also, different buffers were used in these attempts and, in all of them, the sample buffer was the same as the run buffer. In regard to the equipment, the capillary's length was 80cm (total length), which affected, mostly, the running time and the polarity used was normal, except for once, when it was inverted (method 1.1.1.).

### A1.1. Method 1

The first attempt consisted in using a different set of conditions, including the use of a different buffer (which played both roles- sample and run buffer). This methodology (the first one put to use) was dismissed due to the results obtained- both analytes yielded peaks that differed greatly from what was expected, however, the results obtained when analyzing the ssDNA were the ones that lead us to discard this protocol, since this analyte presented a detection time of around 35min and, after 70min, one could still see peaks forming.

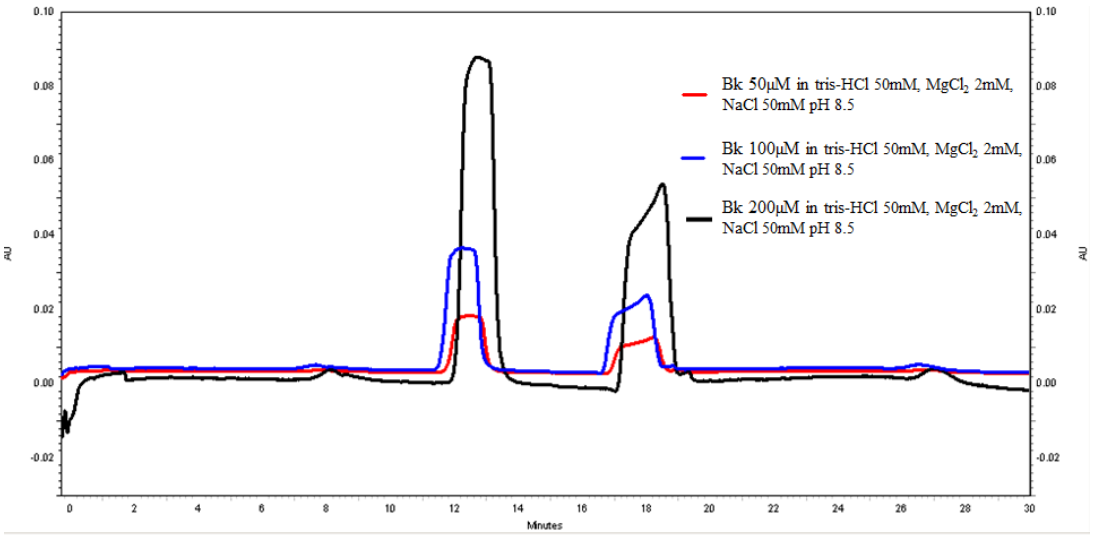


**Figure 31– 3 runs of Bk in different concentrations**. Three different concentrations of Bk were used- 200, 100 and 50uM- all in tris-HCl 50mM, $MgCl_2$ 2mM, NaCl 50mM pH 8.5.

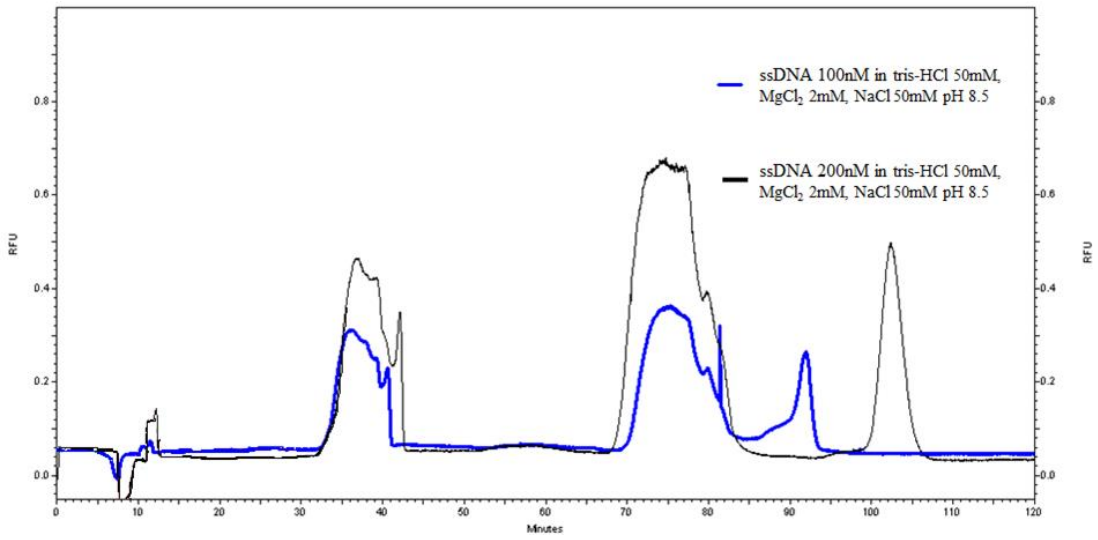


**Figure 32– 2 runs of ssDNA with two different concentrations**. Two different concentrations were used- 100nM and 200nM- all in tris-HCl 50mM, $MgCl_2$ 2mM, NaCl 50mM pH 8.5.

### A1.1.1. Reversed Polarity

Changing the polarity was, also, part of the development process (whilst maintaining the capillary length and the buffer). However, the results yielded proved that this was, definitely, not the right path, since no signal was obtained.

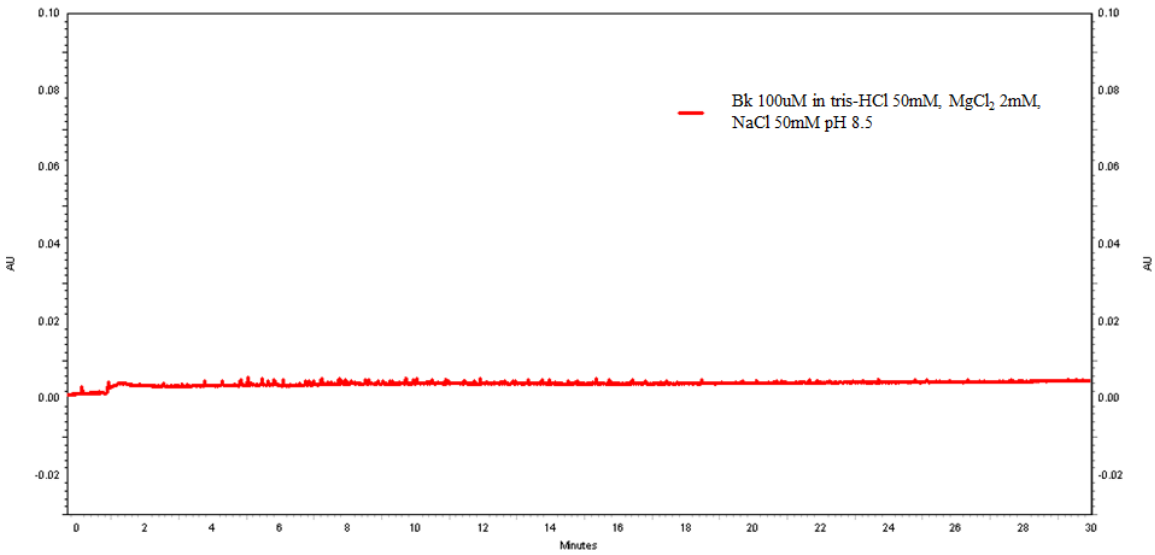


**Figure 33 – Bk run with reversed polarity.** 100µM Bk in 50mM tris-HCl, 2mM $MgCl_2$, 50mM NaCl pH 8.5. No signal was obtained.

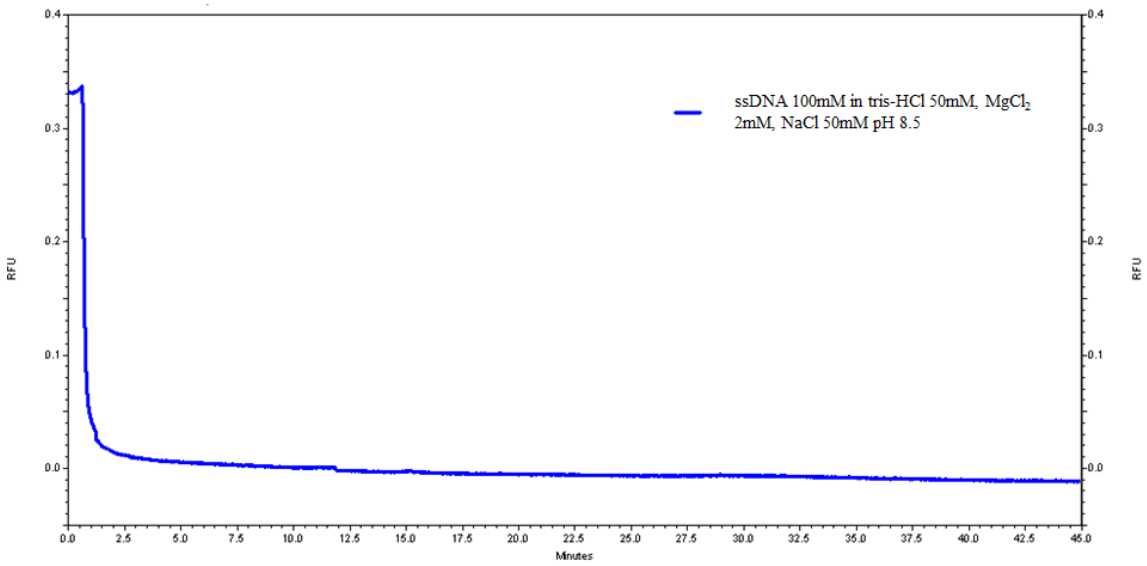


**Figure 34– ssDNA run with reversed polarity**. 100nm ssDNA in tris-HCl 50mM, $MgCl_2$ 2mM, NaCl 50mM pH 8.5. No signal was obtained.

## A1.2. Method 2

PBS buffer was also tried. In this case, the time frames didn't allow for a useful collection window, since the target's peak detection window lies within that of the ssDNA. As before, the sample buffer and the separation buffer were both the same- 136.8mM NaCl, 44.8mM $NaH_2PO_4$, 26.8mM KCl, 14.6mM $KH_2PO_4$ pH 7.4

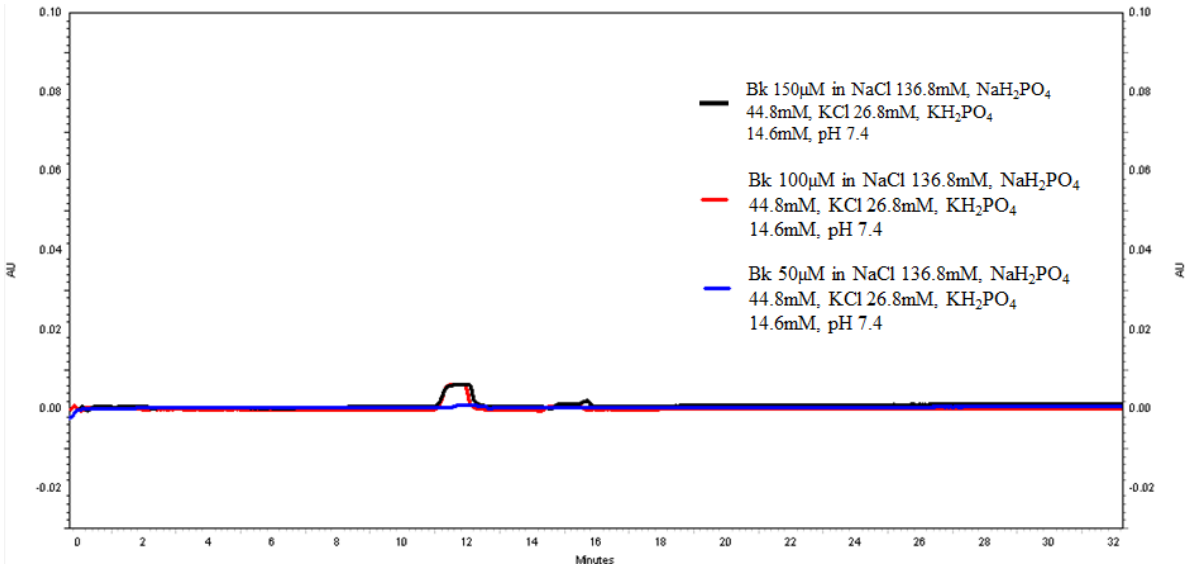


**Figure 35– 3 runs of Bk in different concentrations**. 3 different concentrations were used- 50, 100 and 150uM- in PBS buffer (136.8mM NaCl, 44.8mM $NaH_2PO_4$, 26.8mM KCl and 14.6mM $KH_2PO_4$, pH 7.4). The end of the detection time coincides with that of the ssDNA, thus making it impossible to define a collection window.

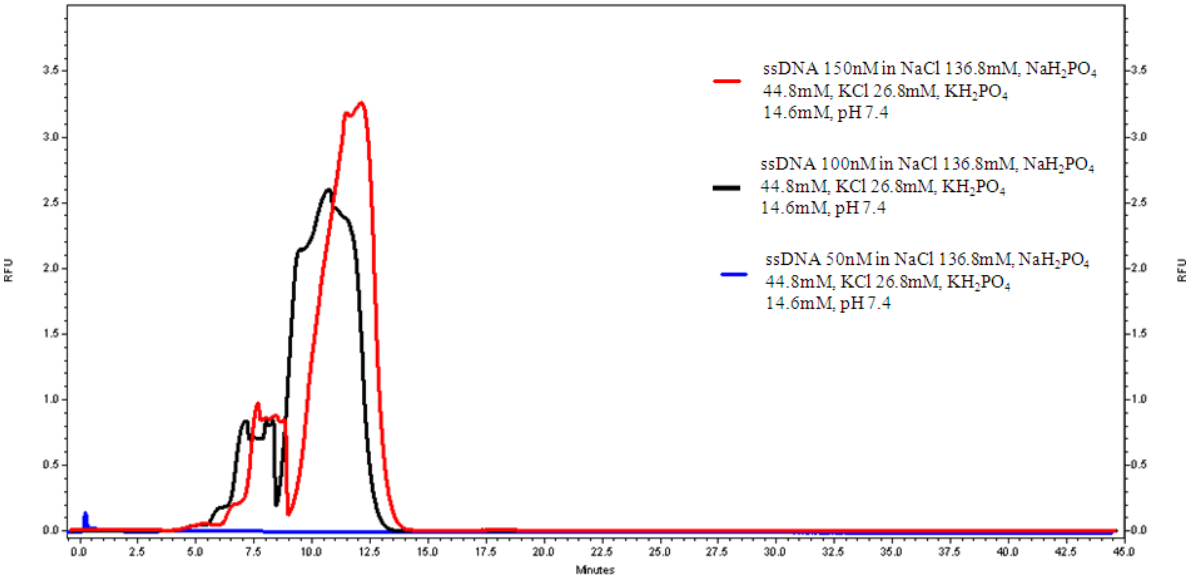


**Figure 36 – 3 runs of ssDNA in different concentrations**. 3 different concentrations were used- 50, 100 and 150nM- in PBS buffer (136.8mM NaCl, 44.8mM $NaH_2PO_4$, 26.8mM KCl and 14.6mM $KH_2PO_4$, pH 7.4). The end of the detection time coincides with that of the target, thus, making it impossible to define a collection window.

.

## A1.3. Method 3

A buffer containing HEPES (4-(2-hydroxyethyl)-1-piperazineethanesulfonic acid) was also used- 25mM HEPES , 1.4mM KCl, 1.8mM $CaCl_2$-$2H_2O$, 1.2mM $MgCl_2$, 145mM NaCl, pH 7.4.

The target's peaks were rather large and the EOF was quite noticeable. The reason why it was discarded was that he ssDNA yielded rather unreproducible results.

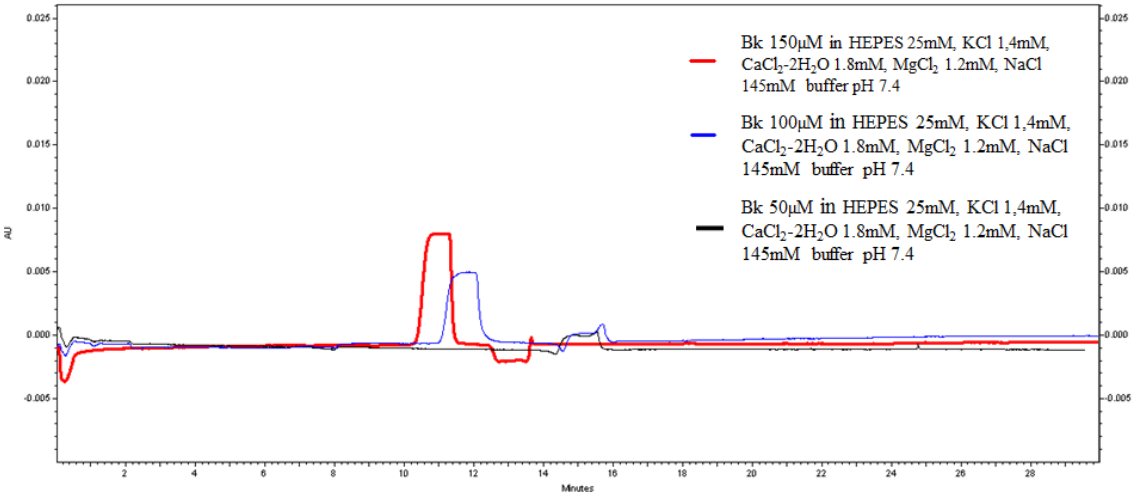


**Figure 37– 3 different target runs with different concentrations**. Bk was analyzed in 3 different concentrations- 50, 100 and 150uM- in 25mM HEPES , 1.4mM KCl, 1.8mM $CaCl_2$-$2H_2O$, 1.2mM $MgCl_2$, 145mM NaCl, pH 7.4

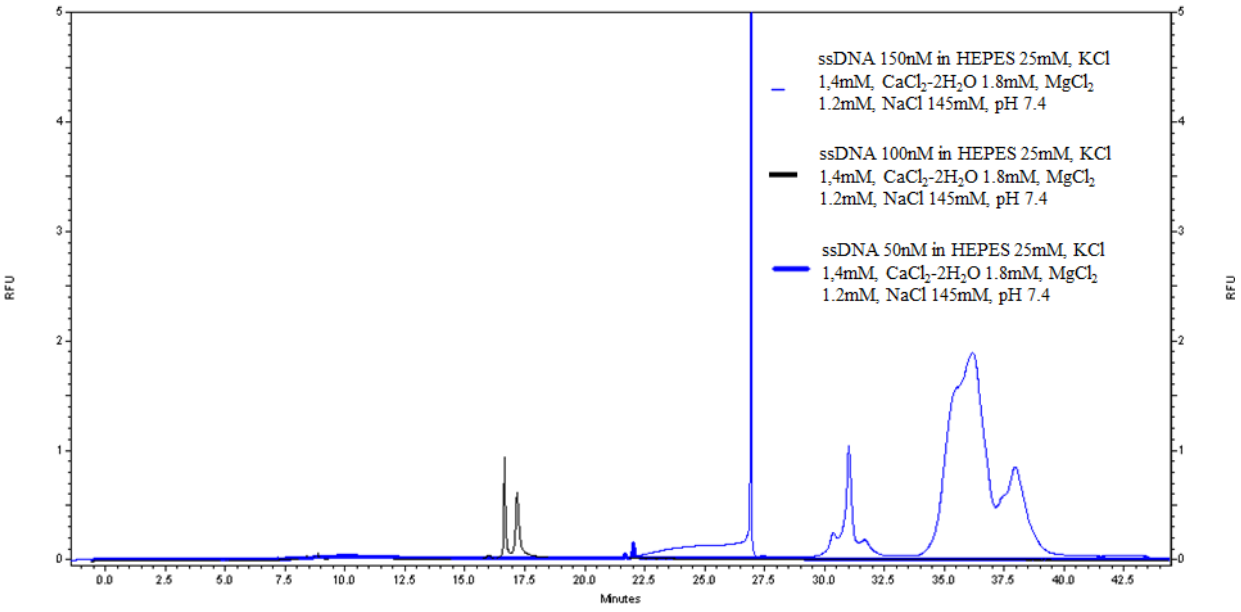


**Figure 38 - 3 different ssDNA runs with different concentrations**. The DNA was analyzed in 3 different concentrations- 50, 100 and 150uM- in 25mM HEPES , 1.4mM KCl, 1.8mM $CaCl_2$-$2H_2O$, 1.2mM $MgCl_2$, 145mM NaCl, pH 7.4. The peaks profile variation is quite noticeable- one of the runs is an almost flat line, whilst the other two have very different peak distribution.

### A1.4. Method 4

Another interesting result obtained during the course of this process was the one presented below. It resulted from the use of the buffer proposed by S. Krylov for this type of aptamer selection[47]. Regarding the target, the analysis didn't reveal to be much efficient. In regard to the ssDNa, no peaks were observed.

Regarding the library, the buffer turned out to be inefficient, since no peaks were detected.

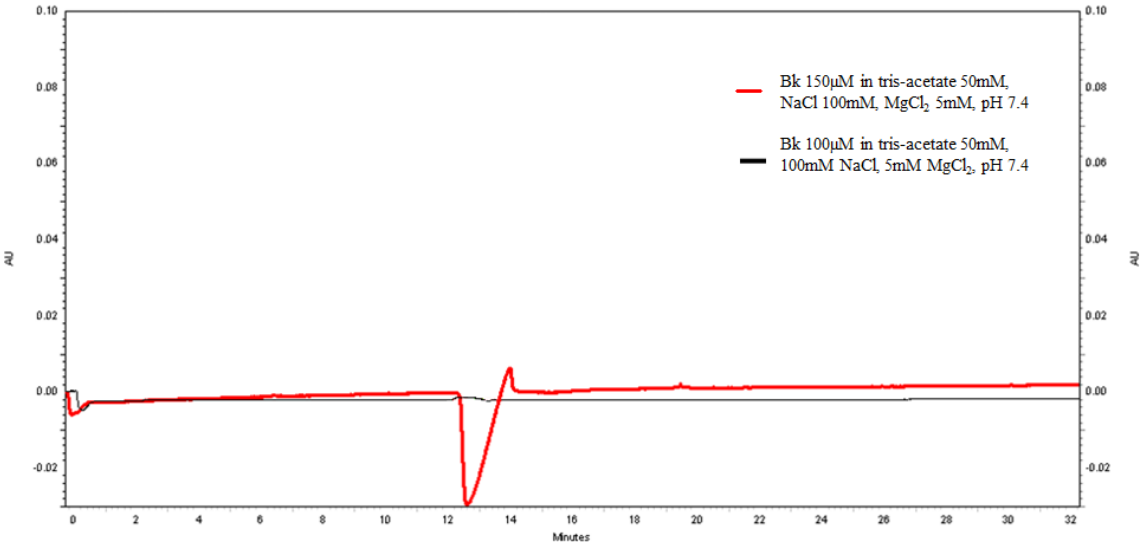


**Figure 39 – Two Bk runs with different concentrations- 100 and 150uM**. The buffer used was tris-acetate 50mM, 100mM NaCl, 5mM $MgCl_2$, pH 7.4.

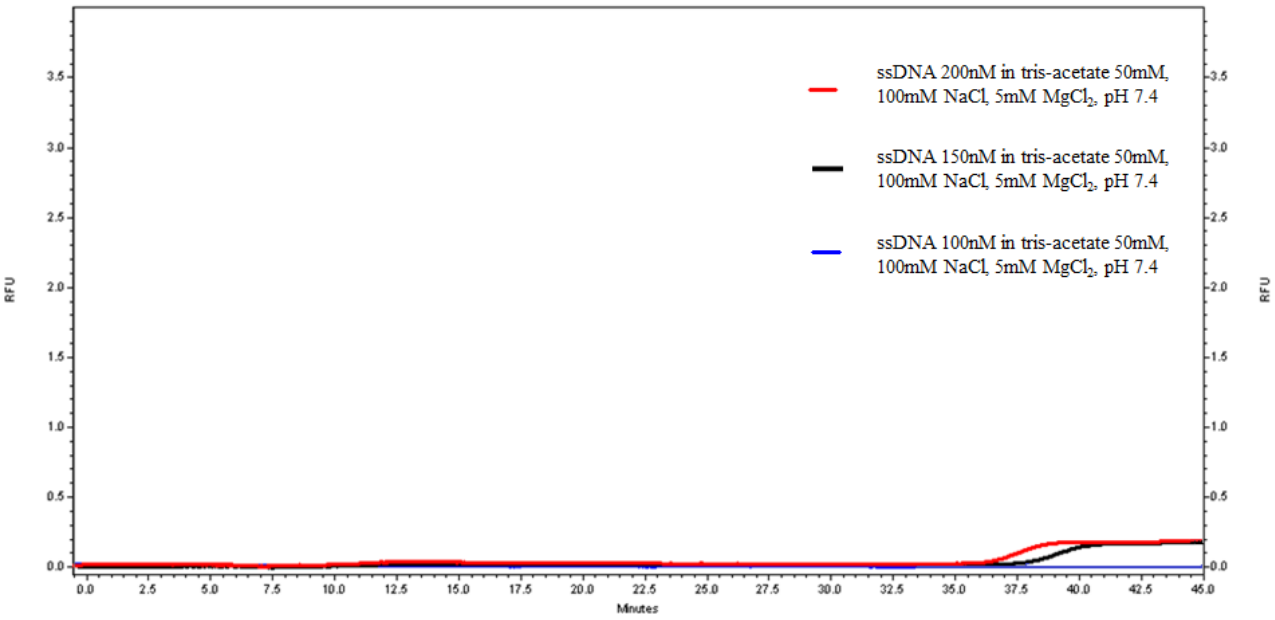


**Figure 40 – 3 ssDNA runs with varying concentrations- 100, 150, 200nM**. The buffer used was tris-acetate 50mM, 100mM NaCl, 5mM $MgCl_2$, pH 7.4. No peaks were obtained.

.

### A1.5. Method 5

This method was, apart from the one presented in this dissertation, the one that yielded the most interesting results- distinct migration times and bold, solid peaks which revealed high reproducibility. In spite of the results obtained, this buffer had to be discarded because both analytes had the same migration times. Both buffers- run buffer and sample buffer- were the same- 150mM NaCl, 4mM $MgCl_2$, 10mM tris-HCl, pH 7.4.

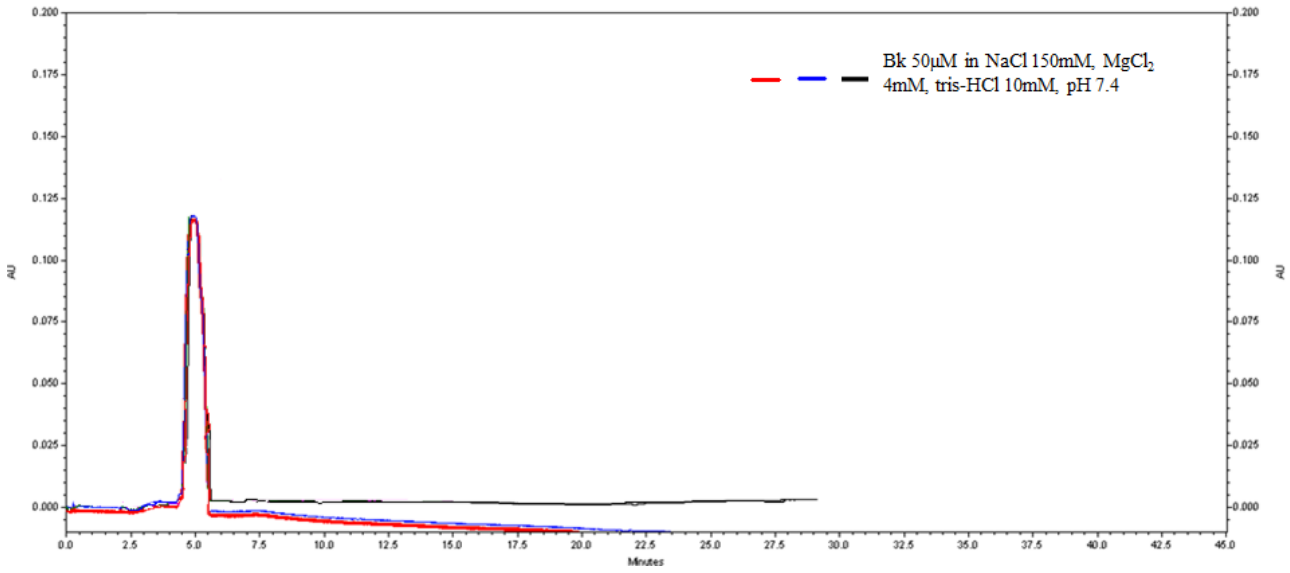


**Figure 41 – 3 Bk runs in NaCl 150mM, $MgCl_2$ 4mM, tris-HCl 10mM, pH 7.4.**

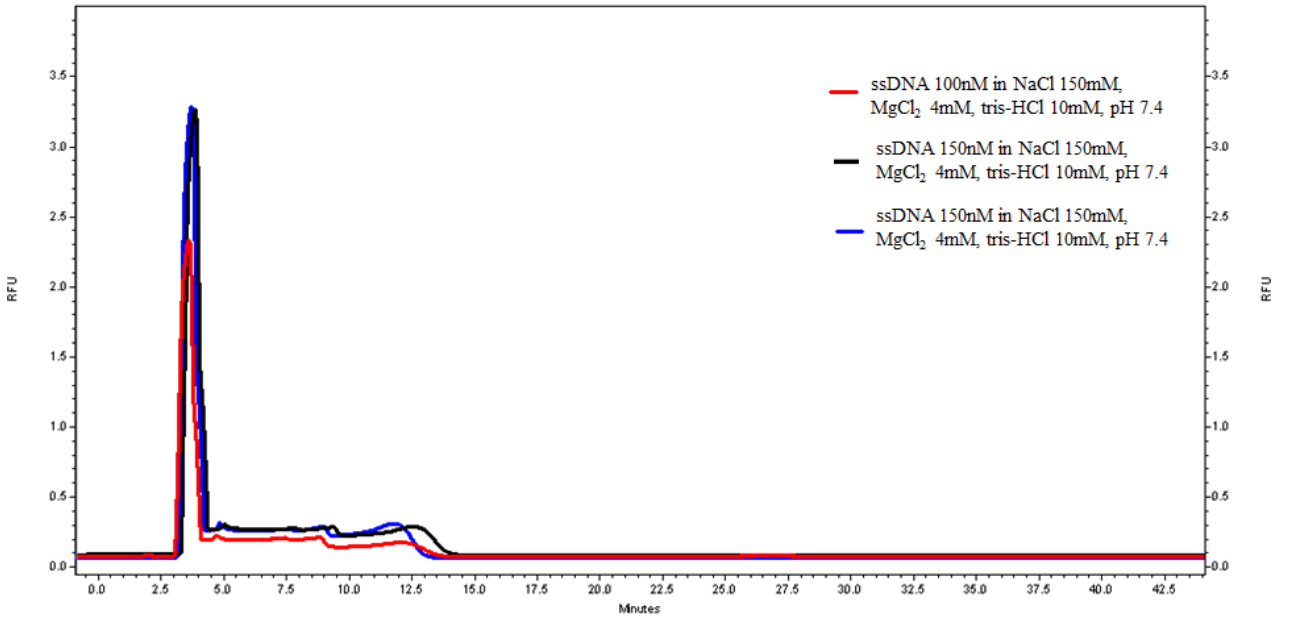


**Figure 42 – 3 ssDNA runs with varying concentrations**. The ssDNa was analyzed using 3 different concentrations- 100 and 150nM- in NaCl 150mM, $MgCl_2$ 4mM, tris-HCl 10mM, pH 7.4. The migration times are almost the same as the ones seen in the target's analysis (previous figure).